

Role of thermal fluctuations in nucleation of three-flavor quark matter

Mirco Guerrini ^{1,2} , Giuseppe Pagliara ^{1,2} , Andrea Lavagno ^{3,4} , Alessandro Drago ^{1,2} 

¹ Department of Physics and Earth Science, University of Ferrara, 44122 Ferrara, Italy

² INFN, Sezione di Ferrara, 44122 Ferrara, Italy

³ Department of Applied Science and Technology, Politecnico di Torino, 10129 Torino, Italy

⁴ INFN Sezione di Torino, 10125 Torino, Italy

* correspondence: mirco.guerrini@unife.it

Abstract: We present a framework that aims to investigate the role of thermal fluctuations of the matter composition and color-superconductivity in the nucleation of three-flavor deconfined quark matter in the typical conditions of high-energy astrophysical systems related to compact stars. It is usually assumed that the flavor composition is locally fixed during the formation of the first seed of deconfined quark matter since weak interaction acts too slowly to re-equilibrate flavors. However, the matter composition fluctuates around its average equilibrium values at the typical temperatures of high-energy astrophysical processes. Here, we extend our previous two-flavor nucleation formalism to a three-flavor case. We develop a thermodynamic framework incorporating finite-size effects and thermal fluctuations of local composition to compute the nucleation probability as the product of droplet formation and composition fluctuation rates. Moreover, we discuss the role of color-superconductivity in nucleation, arguing that it can play a role only in systems larger than the typical coherence length of diquark pairs. We found that thermal fluctuations of the matter composition lead to lowering the potential barrier between the metastable hadronic phase and the stable quark phase. Moreover, the formation of diquark pairs reduces the critical radius and thus the potential barrier in the low baryon density and temperature regime.

Keywords: dense QCD, nucleation, compact stars, strange matter

1. Introduction

The possibility of formation of quark matter in compact stars is usually modelled as a first order phase transition which is triggered by the nucleation of a first drop of quark phase in the hadronic medium. Many papers have addressed this issue trying to estimate the probability of nucleation in several astrophysical conditions, namely for different values of the temperature and baryon density, different types of compositions (two-flavor or three flavor quark matter, hadronic matter with or without hyperons), different models for the dense matter equation of state [1–5]. Also, the effect of color-superconductivity in quark matter has been studied, see e.g. [6]. Finding the threshold for the quark nucleation process (namely the condition for which the nucleation time is comparable to the dynamical time scale) is crucial for addressing the possibility of the occurrence of deconfinement in the formation of hybrid stars (HS) in protoneutron stars (PNS) and in the merger of two compact stars (BNSM), see e.g. [7]. Moreover, also in the case in which strange quark matter (SQM) is absolutely stable (and thus, at least some compact stars are actually strange quark stars), a correct determination of the nucleation threshold is key for understanding at which conditions compact stars can convert into strange quark stars (Qs) leading to the scenario in which hadronic stars and strange quark stars coexist (the so-called two-families scenario, [8–10]).

A key issue, when computing nucleation in multicomponent systems, concerns the concentrations of the several species of particles in the metastable phase and in the new phase. In the seminal paper [1] it is argued that the energy fluctuation leading to the formation of a stable droplet of the quark phase occurs on a time scale which is of the order of the time scale of strong interaction, namely $\sim 10^{-23}$ s. During this tiny amount of time,



Citation: Guerrini, M.; Pagliara, G.; Lavagno, A.; Drago, A. Role of thermal fluctuations in nucleation of three-flavor quark matter. *Preprints* 2025, 1, 0. <https://doi.org/>



Copyright: © 2025 by the authors. Licensee MDPI, Basel, Switzerland. This article is an open access article distributed under the terms and conditions of the Creative Commons Attribution (CC BY) license (<https://creativecommons.org/licenses/by/4.0/>).

there is no chance that the composition of matter can change due to the occurrence of weak interactions, which are much slower. Thus, the flavor composition is frozen during the nucleation, and the droplets of quark matter have the same concentrations of up, down and strange quarks of the hadronic metastable phase. Since the flavor compositions of hadronic matter and quark matter in β -equilibrium are different (especially when considering strangeness), the first droplet of quark matter would be in an out-of-equilibrium phase. The effect of this assumption is to substantially increase the baryon density at which quark matter appears with respect to the stationary situation of thermodynamical equilibrium in which the two phases are in mechanical, chemical, and thermal equilibrium. In our recent work [11], we have revised the standard formalism of nucleation in multicomponent systems by introducing the possibility of thermal fluctuations of the composition of the different species of particles in the case of two-flavor quark matter. The fluctuations we consider in that work basically correspond to the density fluctuations within the grandcanonical ensemble of statistical mechanics that are in no way related to the action of weak interactions but are related instead to the fact that the droplet of quark matter is immersed in a large "bath" of hadronic matter that behave as a source of energy and a source of particles for the quark matter droplet. As a result, by considering those kinds of fluctuations, the nucleation process is much more efficient with respect to the case of frozen composition. In this paper, we will extend the formalism developed in [11] to the case of three-flavor quark matter. In particular, we will consider hadronic equations of state (EOSs) which include hyperons (hadronic matter with finite net strangeness) and two types of strange quark matter equations of state: i) unpaired quark matter and ii) color-flavor locked (CFL) quark matter, one of the possible candidates for color-superconductivity in compact stars [12–14]. Indeed, it has been suggested that color-superconductivity is crucial for the astrophysical phenomenology, since the existence of a candidate compact star with a mass of $\sim 2.6M_\odot$ [15,16] suggests that the EOS of dense matter is rather stiff. This applies both for hybrid stars in the standard one family scenario (see e.g. [17–19]) and for quark stars (QS) within the two families scenario (see e.g. [20]). Moreover, color-superconducting phases could set in only if the droplet of the quark phase is large enough to allow for the creation of the diquark pairing correlation, whose typical size is of the order of $\sim 1/\Delta$ [13]. In this respect, as we will show, the critical radius for the formation of a stable quark matter droplet could be strongly affected by the possibility of the formation of the CFL phase.

The paper is organized as follows: in Sec. 2, nucleation formalism considering thermal fluctuations of the hadronic composition will be presented in detail. In Sec. 3 we will describe our framework that aims to include the role of color-superconductivity. Our results will be highlighted in Sec. 4. A summary and the conclusions will be reported in Sec. 5. Finally, in Appendix A, the EOS models used will be presented.

We will use natural units $\hbar = c = 1$ and $k_B = 1$.

2. Nucleation theory

Let us consider a closed system with two stable equilibrium solutions: a pure metastable hadronic phase H (corresponding to an energy local minimum) and a stable pure deconfined quark phase Q (corresponding to the energy global minimum). Let us prepare initially the system in the metastable hadronic phase H at a temperature T . Due to thermal or quantum fluctuations, the system continuously explores configurations around the local minimum (and thus, the thermodynamical quantities around their equilibrium average values). The probability of a generic thermal fluctuation is [21]

$$\mathcal{P} \propto e^{-W/T}, \quad (1)$$

where W is the energy difference between the fluctuated and the equilibrium configurations, corresponding to the work needed to pass from one configuration to the other with a reversible transformation. The larger the temperature, the larger the probability of having large fluctuations with respect to the minimum. The available configurations depend on the kinds of reactions that can occur. For example, if only strong interactions occur, the

global flavor composition can not be modified. On the other hand, if weak reactions are also involved, configurations with different flavor compositions with respect to the initial equilibrium can be explored.

We are, in particular, interested in studying the phase transition between the local and global minima, namely the deconfinement of quarks from hadrons in dense matter. Fluctuations can locally produce small droplets of the deconfined quark phase. The most likely path in the configuration space to pass from the local to the global minima is the one that passes near the lowest intervening saddle point of the potential between the phases H and Q [22,23]. In our picture, this saddle point describes a configuration in which the system is all in the metastable hadronic phase except for a single critical droplet of the stable deconfined quark phase. Namely, the saddle point is a local maximum of the potential as a function of the volume occupied by the quark droplet, thus a mechanically unstable equilibrium configuration. This arises from the competition between a negative bulk term, which scales with the volume of the new quark phase, and a positive surface term related to the surface tension, which scales with its interfacial area. The quantity $W = E_{sp} - E_H$ between the energy of the saddle point configuration E_{sp} and the energy E_H of the metastable H state represents the height of the potential barrier (usually called "activation energy") that separates the two minima H and Q . Thus, if a fluctuation generates a droplet of the deconfined quark phase with a volume smaller than the critical one, the droplet is mechanically unstable and disappears. However, if the generated droplet is as large as or larger than the critical one, the potential barrier is overcome, and the whole system will relax in the new stable phase Q . This process is usually referred to as nucleation¹ and it is the trigger for a first-order phase transition. The rate (number of critical-sized droplets created in unit volume in unit time) at which the potential barrier is overcome by a thermal fluctuation is [22,23]

$$\Gamma = \Gamma_0 e^{-W/T}, \quad (2)$$

where Γ_0 is a prefactor that will be discussed further on. Finally, the nucleation time, namely the typical timescale after which a thermal nucleation event happens, is

$$\tau = \frac{1}{V\Gamma}, \quad (3)$$

where Γ is the nucleation rate in Eq. (2) and V the volume of the system. In the context of compact stars, in principle, one should compute the local nucleation rate at all points of the star where the hadronic phase is metastable and then integrate over the volume. However, a standard choice is to identify the total volume of the system as the innermost stellar region characterized by a sphere of radius ~ 100 m where thermodynamic quantities are almost constant (see e.g. [3,4]), assuming that the contribution of the rest of the star is negligible. Namely, $V \sim 10^{51} \text{ fm}^3$.

Note that this formalism is general for the decay of a metastable state into a stable one and does not assume other specific features of the system (e.g., it does not assume that the droplet is a localized accumulation of particles and it can also apply, for example, to the onset of superfluid phases by the formation of a sufficiently large vortex ring) [22,23].

An alternative path for the nucleation process is quantum nucleation, in which the potential barrier is overcome through quantum tunnelling. It has been shown that at low temperatures ($T \lesssim 10$ MeV), quantum nucleation becomes more efficient than thermal nucleation [3,11]. An estimate of the quantum nucleation rate can be found in [5,24]. However, in this work, we will focus on thermal nucleation, which is more efficient for the typical temperatures of PNSs, CCSNe, and BNSMs.

¹ In principle, nucleation can be either inhomogeneous or homogeneous. The former is more common in nature and occurs when an impurity triggers the phase transition. However, we are here interested in homogeneous nucleation, where the phase transition is triggered by an intrinsic phenomenon, namely by a thermodynamical fluctuation.

The correct individuation of the saddle point configuration E_{sp} is a key element for the computation of the activation energy and the nucleation time. Let us begin by considering which configurations can be explored by the system through thermal fluctuations. The typical timescale of a fluctuation in the volume of the quark matter phase within the state H is the typical time over which a mechanically unstable droplet is created, shrinks back to the metastable phase, and disappears to restore the equilibrium of the system. The timescale for generating a critical droplet is set by the time needed to reach the saddle point configuration by means of a thermal fluctuation. Being deconfinement a strong-interaction mediated phase transition, and since the weak interaction timescale is many orders of magnitude longer than the strong interaction timescale ($\tau_{strong} \sim 10^{-24}$ s), we can assume that only strong interaction is "turned on" and is thus responsible for the fluctuation generating the critical droplet. Consequently, the conserved quantities will be the baryon number B , the non-leptonic electromagnetic charge² C , the strangeness S and the leptonic number L . Note that the first three numbers can be remapped into the three quark flavors u, d, s that are indeed conserved by strong reactions. While this assumption is generally accepted in the literature on quark nucleation, it is debated whether B, C, S, L are locally or globally conserved. As suggested by [25–27], the total free energy is minimized if the two phases can share the conserved numbers. Thus, numbers conservations are global (and not local) unless the reactions that exchange conserved numbers from one phase to the other are suppressed because of some microphysical mechanisms. These mechanisms could include charge screening effects caused by long-range forces, the slowness of specific reactions, or the suppression of diffusion processes. A comprehensive microscopic treatment should consider all the rates of strong reactions responsible for forming the critical droplet and exchanging conserved numbers between the droplet and its surroundings. However, those calculations can be simulated within a thermodynamical approach in two limiting cases³: (i) local flavor conservation: exchange of conserved numbers between the droplet and the surrounding is suppressed; (ii) global flavor conservation: conserved numbers are in strong chemical equilibrium between the droplet and the surrounding. In the former (latter) limit, the equilibration time for the exchange of strong conserved numbers between the quark droplet and the surroundings is much longer (shorter) than the timescale of formation of the critical droplet.

In [3] (and references therein), the local number conservation (frozen flavor composition) is assumed for quark nucleation. On the other hand, in some works addressing the effect of phase transitions in heavy-ion collisions, a global number conservation is assumed. For example, in [29–31] the strangeness is globally (and not locally) conserved leading to the so called "strangeness distillation" effect. The same approach, but with global isospin conservation, has been used in [32].

Another aspect, disregarded in [3], concerns the thermal statistical fluctuation of the particle composition at finite temperature, which could also impact the efficiency of nucleation, as discussed in [4,32,33]. In this work, we will use the approach presented in [11]: let us assume that the conserved number k cannot be exchanged with the surrounding (local conservation of number k). Thus, the critical droplet of deconfined quarks will have the same fraction of k as the preexisting hadronic phase. However, at finite temperature T , the composition $\{Y_k^H\}$ of the initial phase must be considered as a bulk average value. Locally, thermodynamic quantities fluctuate around such average values. Being nucleation a local phenomenon, the first critical droplet of deconfined quark matter could be produced in a small subsystem of the initial hadronic system in which the composition $\{Y_i^*\}$ is different with respect to the average values $\{Y_i^H\}$ and more favorable for the nucleation.

² Namely, the electromagnetic charge of hadrons and quarks. For example, in pure nucleonic matter, this number equals the proton number. This conserved number can be replaced with the isospin.

³ In [28] an intermediate approach is adopted in which the electromagnetic charge neutrality is fulfilled partially locally and partially globally. In principle, the same framework could be applied for a partial local and partial global flavor conservation.

In this framework, the total nucleation rate will be

$$\Gamma = \Gamma_0 e^{-\frac{W_1}{T}} e^{-\frac{W_2}{T}}, \quad (4)$$

where the second exponential is the probability of generating a critical droplet of a deconfined quark phase Q_* within a specific fluctuated hadronic subsystem H_* characterized by a composition $\{Y_i^*\}$. While the first exponential is the probability that the subsystem H_* exists in the initial hadronic system [11].

We need now to compute W_1 and W_2 . Let us assume that the initial system has a volume V , it is in the metastable hadronic phase H , with a temperature T , and it is characterized by the numbers $\{N_i^H\}$, where $i = B, C, S, e, \nu_e$ label respectively the baryon number, the non-leptonic electromagnetic number, the strangeness number, the net electrons number and net electronic neutrinos number⁴. It is useful to introduce the number densities $n_i^H = N_i^H/V$, and the number fractions $Y_i^H = N_i^H/N_B^H = n_i^H/n_B^H$. The energy of the initial hadronic phase is

$$E_H = E_H(N_B^H, \{Y_i^H\}, V, T) = V \varepsilon_H(n_B^H, \{Y_i^H\}, T). \quad (5)$$

where ε_H is the energy density. Let us now focus on the saddle point configuration, namely the one in which the system is all in the hadronic phase except for the presence of a single critical spherical droplet of the deconfined quark phase. The two phases are separated by an infinitely small layer, and the energy of the finite-size deconfined quark phase inside the droplet is approximated with a bulk term E_{Q*} plus a surface term E_σ . We will label the quantities inside the droplet with Q_* and in the external hadronic surroundings with \tilde{H} . The energy of this saddle point configuration is

$$E_{sp} = E_{Q*} + E_{\tilde{H}} \quad (6)$$

$$= E_Q(N_B^{Q*}, \{Y_i^{Q*}\}, V_{Q*}, T_{Q*}) + E_\sigma + E_H(N_B^{\tilde{H}}, \{Y_i^{\tilde{H}}\}, V_{\tilde{H}}, T_{\tilde{H}}) \quad (7)$$

$$= V_{Q*} \varepsilon_Q(n_B^{Q*}, \{Y_i^{Q*}\}, T_{Q*}) + E_\sigma + V_{\tilde{H}} \varepsilon_H(n_B^{\tilde{H}}, \{Y_i^{\tilde{H}}\}, T_{\tilde{H}}). \quad (8)$$

In principle, such a critical droplet could be generated at any point in the system. At finite temperature, the thermodynamical quantities of the system are not equal everywhere. The composition $\{Y_i^H\}$ corresponds to an average global composition that could be locally different in different subsystems. Thus, the critical droplet of quark matter can be generated in a subsystem in which the thermodynamical quantities fluctuate with respect to the average equilibrium ones. Let us consider a configuration in which the system is all in the hadronic phase and contains a subsystem H_* characterized by the same baryon number of the critical quark droplet $N_B^{H*} = N_B^{Q*}$ surrounded by a hadronic phase labeled with \tilde{H} .

The energy of this configuration is

$$E_{fl} = E_{H*} + E_{\tilde{H}} \quad (9)$$

$$= E_H(N_B^{H*}, \{Y_i^{H*}\}, V_{H*}, T_{H*}) + E_H(N_B^{\tilde{H}}, \{Y_i^{\tilde{H}}\}, V_{\tilde{H}}, T_{\tilde{H}}) \quad (10)$$

$$= V_{H*} \varepsilon_H(n_B^{H*}, \{Y_i^{H*}\}, T_{H*}) + V_{\tilde{H}} \varepsilon_H(n_B^{\tilde{H}}, \{Y_i^{\tilde{H}}\}, T_{\tilde{H}}). \quad (11)$$

The minimum thermodynamic work W_2 needed to generate a deconfined quark droplet Q_* in a subsystem H_* , assuming a closed system in which the total volume V , numbers $\{N_i^H\}$

⁴ Any linear combination of them that can univocally describe the hadronic phase can also be used. Note that we are at this stage assuming that the initial hadronic phase is in strong equilibrium, namely the composition in terms of hadrons $\{Y_h^H\}$ (where $h = p, n, \Lambda, \Sigma^+, \Sigma^0, \Sigma^-, \Xi^0, \Xi^-, \Delta^{++}, \Delta^+, \Delta^0, \Delta^-$) is fixed by the three numbers B, C, S and the strong equilibrium relations $\mu_h^H = \mu_B^H + C_h \mu_C^H + S_h \mu_S^H$, where C_h, S_h are the C and S charges of hadron h (e.g. $\mu_p = \mu_B + \mu_C, \mu_n = \mu_B, \mu_\Lambda = \mu_B + \mu_S$).

and entropy S_H (since we are interested in the minimum thermodynamic work, namely the adiabatic one [21]) are conserved, is:

$$W_2 = E_{Q^*} + E_{\tilde{H}} - (E_{H^*} + E_{\tilde{H}}) + \sigma S_{Q^*}, \quad (12)$$

where $E_\sigma = \sigma S_{Q^*}$, S_{Q^*} is the surface area of the Q^* droplet and σ the surface tension between the hadronic and quark phases. The surface tension plays a key role in the first-order phase transition by increasing/decreasing the work required to form a quark matter droplet. Nevertheless, its magnitude is highly uncertain, ranging from a few to hundreds of MeV/fm² (see, e.g. [4,5,14,34–39]).

With the same assumptions, the minimum work W_1 for generating the subsystem H_* is

$$W_1 = E_{H^*} + E_{\tilde{H}} - E_H. \quad (13)$$

The conservation relations are

$$V = V_{Q^*} + V_{\tilde{H}} = V_{H^*} + V_{\tilde{H}} \quad (14)$$

$$N_i^H = N_i^{Q^*} + N_i^{\tilde{H}} = N_i^{H^*} + N_i^{\tilde{H}} \quad i = B, C, S, L \quad (15)$$

$$S_H = S_{Q^*} + S_{\tilde{H}} = S_{H^*} + S_{\tilde{H}}. \quad (16)$$

Note that we are choosing the leptonic number $N_L = N_e + N_{\nu_e}$ as conserved number and, in principle, not N_e and N_{ν_e} separately. However, we are dealing here with systems that are charge-neutral (in the sense of electromagnetic charge), namely $N_C^H - N_e^H = 0$. Since N_C^H is conserved in the whole system, N_e^H is also conserved. Thus, given the conservation of N_L and the electromagnetic charge neutrality, N_e^H and $N_{\nu_e}^H$ are actually both conserved separately in the whole system.

Let us assume now that the volume occupied by the deconfined quark droplet and the particle number in it are just small fractions with respect to the total ones: $V \sim V_{\tilde{H}} \sim V_{\tilde{H}} \gg V_{Q^*} \sim V_{H^*}$ and $N_i \sim N_i^{\tilde{H}} \sim N_i^{\tilde{H}} \gg N_i^{Q^*} \sim N_i^{H^*}$. Indeed, the typical critical droplet volume is $V_{Q^*} \sim (100 - 1000) \text{ fm}^3$, while the total volume of the system is $V \sim 10^{51} \text{ fm}^3$. Within this assumption, processes involving the small droplet do not lead to any appreciable change in intensive thermodynamical quantities (μ_i, T, P) of the external hadronic phase, which thus remains nearly equal to the ones in the initial state H [21]. Namely, the surrounding hadronic phase behaves as an external thermal bath and an external reservoir of particles for the deconfined quark droplet Q^* and for the local fluctuated subsystem H_* :

$$P_H \simeq P_{\tilde{H}} \simeq P_{\tilde{H}} \quad (17)$$

$$T \simeq T_{\tilde{H}} \simeq T_{\tilde{H}} \quad (18)$$

$$\mu_i^H \simeq \mu_i^{\tilde{H}} \simeq \mu_i^{\tilde{H}}. \quad (19)$$

Using $E_I = S_I T_I - P_I V_I + \sum_i N_i^I \mu_i^I$ (where $I = Q^*, H_*, \tilde{H}, \tilde{H}, H$), by substituting the conservation relations (Eqs. 14,15,16) in Eq. (12) and Eq. (13), and assuming the equalities in Eqs. (17,18,19) we obtain

$$W_2 = S_{Q^*}(T_{Q^*} - T) + S_{H^*}(T - T_{H^*}) - V_{Q^*}(P_{Q^*} - P_H) - V_{H^*}(P_H - P_{H^*}) + \quad (20)$$

$$+ \sum_i N_i^{Q^*}(\mu_i^{Q^*} - \mu_i^H) + \sum_i N_i^{H^*}(\mu_i^H - \mu_i^{H^*}) + \sigma S_{Q^*} \quad (21)$$

and

$$W_1 = S_{H^*}(T_{H^*} - T) - V_{H^*}(P_{H^*} - P_H) + \sum_i N_i^{H^*}(\mu_i^{H^*} - \mu_i^H). \quad (22)$$

Finally, the total work is

$$W = W_1 + W_2 = E_{Q^*} + E_{\tilde{H}} - E_H + \sigma \mathcal{S}_{Q^*} = \quad (23)$$

$$= S_{Q^*}(T_{Q^*} - T) - V_{Q^*}(P_{Q^*} - P_H) + \sum_i N_i^{Q^*}(\mu_i^{Q^*} - \mu_i^H) + \sigma \mathcal{S}_{Q^*}. \quad (24)$$

Since we are assuming that the quark phase is enclosed in a spherical droplet, we can write $V_{Q^*} = 4/3\pi R_*^3$ and $\mathcal{S}_{Q^*} = 4\pi R_*^2$, where R_* is the radius of the critical droplet (the droplet radius corresponding to the saddle point configuration).

In our framework, the flavor composition of the quark droplet Q_* is equal to the one of the fluctuated subsystem H_*

$$Y_C^{Q^*} \equiv \frac{2}{3}Y_u^{Q^*} - \frac{1}{3}Y_d^{Q^*} - \frac{1}{3}Y_s^{Q^*} = Y_C^{H^*} \equiv Y_C^* \quad (25)$$

$$Y_S^{Q^*} \equiv Y_s^{Q^*} = Y_S^{H^*} \equiv Y_S^*. \quad (26)$$

This choice corresponds to local numbers conservation [27] during quark droplet formation. We are thus assuming that, while strong reactions lead to the generation of a Q_* droplet in the H_* subsystem, strong reactions and diffusion leading to the exchange of C and S between the droplet and the surrounding are suppressed (i.e., the quasiparticles S and C are much slower than the formation of the critical droplet).

By construction, $N_B^{Q^*} = N_B^{H^*} \equiv N_B^*$, and thus $N_i^{Q^*} = N_i^{H^*} \equiv N_i^*$, with $i = C, S$. In principle, Y_C^* and Y_S^* are, at this stage, independent variables. One could remap those variables with the variation with respect to the equilibrium bulk values $Y_i^* = Y_i^H + \Delta Y_i$, (where $i = C, S$). If $\Delta Y_i = 0$, we are back in the standard scenario in which the thermodynamic quantities of the system do not fluctuate and are equal everywhere (see e.g. [40]).

Since we are interested in astrophysical applications, electromagnetic charge neutrality must be imposed. The electromagnetic charge neutrality can be, in principle, locally or globally fulfilled. Which of the two approaches better describes the mixed phase depends on the interplay between the surface tension and the Debye screening length [28,34,41]. Moreover, a complete discussion should consider the contribution of electrostatic energy and compute how leptons distribute to screen the droplet charge [5,24]. However, in this work, we will assume, for simplicity, local charge neutrality.

$$Y_e^{Q^*} = Y_C^{Q^*} = Y_C^* \quad (27)$$

$$Y_e^{H^*} = Y_C^{H^*} = Y_C^*. \quad (28)$$

Moreover, let us assume that the fluctuation in the hadronic system leading to the subsystem H_* occurs in mechanical and thermal equilibrium

$$T_{H^*} = T_{\tilde{H}} = T \quad (29)$$

$$P_{H^*} = P_{\tilde{H}} = P_H. \quad (30)$$

We are thus assuming that in the fluctuation of the hadronic system, mechanical and thermal equilibrium are restored on a negligible timescale, while chemical equilibrium is reached on a longer timescale. Thus, the subsystem H_* will have the same pressure and temperature as the surroundings, but, in general, a different composition $\{Y_i^{H^*}\} \neq \{Y_i^H\}$.

Finally, neutrinos will be considered globally conserved [27] in the system (e.g. in the cases in which they are trapped inside the NS, namely during the first stage of the evolution of a PNS)

$$\mu_{\nu_e}^H = \mu_{\nu_e}^{H^*} = \mu_{\nu_e}^{Q^*} \quad (31)$$

or un-trapped once created (e.g., when the star cooled down, the neutrinos' mean free path becomes larger than the star's size and they are thus free streaming)

$$\mu_{\nu_e}^H = \mu_{\nu_e}^{H*} = \mu_{\nu_e}^{Q*} = 0 \quad (32)$$

In the latter case, the lepton number is no longer conserved. As we will see (see also [27]), in both cases, neutrinos can be handled as an independent contribution to EOS.

Using all these conditions, the works W_1 , W_2 , W becomes

$$W_1 = \sum_{i=B,C,S,e} N_i^* (\mu_i^{H*} - \mu_i^H) \quad (33)$$

$$= \frac{4}{3} \pi R_*^3 n_B^{Q*} \sum_{i=B,C,S,e} Y_i^* (\mu_i^{H*} - \mu_i^H) \quad (34)$$

$$W_2 = S_{Q*} (T_{Q*} - T) - V_{Q*} (P_{Q*} - P_H) + \sum_{i=B,C,S,e} N_i^* (\mu_i^{Q*} - \mu_i^{H*}) + \sigma S_{Q*} \quad (35)$$

$$= \frac{4}{3} \pi R_*^3 \left[s_{Q*} (T_{Q*} - T) - (P_{Q*} - P_H) + n_B^{Q*} \sum_{i=B,C,S,e} Y_i^* (\mu_i^{Q*} - \mu_i^{H*}) \right] + 4\pi\sigma R_*^2 \quad (36)$$

$$W = W_1 + W_2 \quad (37)$$

$$= S_{Q*} (T_{Q*} - T) - V_{Q*} (P_{Q*} - P_H) + \sum_{i=B,C,S,e} N_i^* (\mu_i^{Q*} - \mu_i^H) + \sigma S_{Q*} \quad (38)$$

$$= \frac{4}{3} \pi R_*^3 \left[s_{Q*} (T_{Q*} - T) - (P_{Q*} - P_H) + n_B^{Q*} \sum_{i=B,C,S,e} Y_i^* (\mu_i^{Q*} - \mu_i^H) \right] + 4\pi\sigma R_*^2, \quad (39)$$

where s_{Q*} is the entropy density.

For a specific EOS for quark matter, P_{Q*} , s_{Q*} , μ_i^{Q*} can be computed as a function of $(n_B^{Q*}, \{Y_i^{Q*}\}, T_{Q*})$, while μ_i^{H*} can be computed as a function of $(n_B^{H*}, \{Y_i^{H*}\}, T_{H*})$ ⁵.

Using the local C and S conservation in the droplet formation (Eqs. 25,26), the electromagnetic charge neutrality (Eqs. 27,28), the mechanical (Eq. 30) and thermal (Eq. 29) equilibrium of the hadronic fluctuation and the trapped (or un-trapped) neutrinos condition (Eq. 31 or 32), we are left with the following independent variables: n_B^{Q*} , R_* , $\{Y_i^*\}$ (or equivalently $\{\Delta Y_i\}$) and T_{Q*} , other than the input variables of the initial system n_B^H , $\{Y_i^H\}$, T ⁶.

For the moment, let us keep $\{Y_i^*\}$ as independent variables. The goal is thus to fix somehow the remaining non-input independent variables n_B^{Q*} , R_* and T_{Q*} .

Usually (see e.g. [4,21,22,40]), it is assumed that the droplet of deconfined quarks is in thermal equilibrium with the surrounding

$$T_{Q*} = \tilde{T} = T \quad (40)$$

namely, thermal equilibrium is reached in a negligible timescale during the formation of the critical droplet. One can easily note that, under this assumption, the minimum work required to jump from one configuration to another is the difference between the free energies $F = E - ST$ of the two configurations.

⁵ Note that, while $N_i^{H*} = N_i^{Q*} \equiv N_i^*$ and $Y_i^{H*} = Y_i^{Q*} \equiv Y_i^*$, we still have $n_B^{H*} \neq n_B^{Q*}$, since in general $V_{H*} \neq V_{Q*}$.

⁶ Even if here we are in general considering $\{Y_i^H\}$ as input, they are sometimes fixed by n_B^H , (Y_L^H) and T , for example if the initial system is in β -equilibrium without (with) trapped neutrinos. On the other hand, Y_C^H (e.g. in CCSNe [42]) and/or Y_S^H (e.g. in heavy-ion collisions) remain independent variables if the dynamical timescale is shorter than the equilibration timescale of leptonic weak interaction and non-leptonic weak interaction, respectively (see [27,42]).

Let us explore some possibilities for fixing the other two variables:

2.1. Small degrees of metastability

In [11], we used the "small degree of metastability" [21] approximation as in [3]. The system has a "low degree of metastability" if:

$$\delta P_H = |P_H - P_x| \ll P_x \quad (41)$$

$$\delta P_{Q^*} = |P_{Q^*} - P_x| \ll P_x, \quad (42)$$

where P_x is the pressure at the equilibrium when $R_* \rightarrow +\infty$ (plane surface) or $\sigma \rightarrow 0$, so that

$$\mu_k^H(P_x, T) = \mu_k^Q(P_x, T), \quad (43)$$

where k labels every globally conserved charge and μ_k the associated chemical potential. Namely, P_x is the equilibrium pressure of the two phases in a first-order phase transition at temperature T in bulk. In other words, a system has a low degree of metastability if the overpressure needed in the metastable phase to balance the finite-size effects due to the surface tension is relatively small.

Thus, within this approximation, we can set the equation:

$$P_{Q^*} \simeq P_H \quad (44)$$

and substituting it as equality together with Eq. (40) in Eqs. (36) and (39) and obtain:

$$W_2 = \frac{4}{3} \pi R_*^3 n_B^{Q^*} \left[\sum_{i=B,C,S,e} Y_i^* (\mu_i^{Q^*} - \mu_i^{H^*}) \right] + 4\pi\sigma R_*^2, \quad (45)$$

$$W = \frac{4}{3} \pi R_*^3 n_B^{Q^*} \left[\sum_{i=B,C,S,e} Y_i^* (\mu_i^{Q^*} - \mu_i^H) \right] + 4\pi\sigma R_*^2, \quad (46)$$

where $n_B^{Q^*}$ is fixed using the equality in Eq. (44).

Note that $\sum_i Y_i^* (\mu_i^{Q^*} - \mu_i^{H^*})$ is equal to $\mu_{Q^*} - \mu_{H^*}$, where $\mu_I = \sum_i Y_i^I \mu_i^I = (P_I + \varepsilon_I - s_I T_I) / n_B^I$ is the Gibbs energy per baryon in the phase I , but computed without neutrinos contributions. Moreover, in absence of hadronic composition fluctuations ($Y_i^* = Y_i^H$ for $i = C, S$), we have $\sum_i Y_i^* (\mu_i^{Q^*} - \mu_i^H) = \mu_{Q^*} - \mu_H$ again, computed without neutrinos.

Let us now focus on fixing R_* . In [11] we computed it as the droplet radius that maximizes W_2 . However, this approach actually underestimates R_* . Indeed, R_* must correspond to a mechanically unstable configuration such that, once it is overcome by a δR , the whole system is free to reach the absolute minimum of the potential. However, a droplet with a radius R_2 (such that $\max W_2 = W_2(R_2)$) would not have this feature. Once a droplet with radius R_2 is formed, a subsystem H_* characterized by number of baryons $N_B^* = \frac{4}{3} \pi R_2^3 n_B^{Q^*}$ and a compositions $\{Y_i^*\}$ has been converted into a deconfined quark Q_* droplet. However, the surrounding is in the $\tilde{H} \simeq H$ configuration, and not in H_* , thus it is not necessarily energetically convenient for the quark droplet to increase its radius by a δR and absorb other baryons. Indeed, the Q_* phase is energetically favorable with respect to H_* , but not with respect to H . Namely $\mu_{Q^*} < \mu_{H^*}$ but $\mu_{Q^*} > \mu_H$ at fixed P and T .

One can easily note that the requested feature for the critical radius is fulfilled by a value of R_* such that $\max W = W(R_*)$. A configuration having a deconfined droplet with a radius R_* is in a phase Q_* that, even adding the surface tension term, is more stable than the surrounding matter $\tilde{H} \simeq H$.

Thus, R_* corresponds to the maximum of W (and not of W_2), namely

$$R_* = \frac{2\sigma}{n_B^{Q^*} \left[\sum_{i=B,C,S,e} Y_i^* (\mu_i^H - \mu_i^{Q^*}) \right]} \quad (47)$$

and it exists only if $\sum_{i=B,C,S,e} Y_i^* (\mu_i^H - \mu_i^{Q*}) > 0$. The total work W is thus

$$W = \frac{16\sigma^3}{3} \frac{1}{\left[n_B^{Q*} \sum_{i=B,C,S,e} Y_i^* (\mu_i^H - \mu_i^{Q*}) \right]^2}. \quad (48)$$

2.2. Saddle-point approach

This approach states that n_B^{Q*} is not fixed by any physical condition, and thus, it can have, in principle, any value, indicating how big (in terms of baryon number $N_B^* = n_B^{Q*} V_{Q*}$) the fluctuation is. In this subsection, we will still consider T_{Q*} as a free variable, as the condition $T_{Q*} = T$ will naturally emerge in the calculations.

In the spirit of the saddle-point approach (the most likely path in the configurations space to pass from the local to the global minima is the one that passes near the lowest intervening saddle point of the potential [22,23]), we will choose the R_* that maximizes W (unstable mechanical equilibrium) and the n_B^{Q*} and T_{Q*} that minimizes it. The reason is that being n_B^{Q*} and T_{Q*} in principle free, one should compute the total probability of nucleating as an integral over all the possible n_B^{Q*} and T_{Q*} , but, being the probability a negative exponential of W/T , the contributions related to the n_B^{Q*} and T_{Q*} that minimizes W will dominate.

By minimizing W (Eq. 39) with respect to T_{Q*} we obtain the thermal equilibrium condition

$$T_{Q*} = T, \quad (49)$$

while minimizing with respect to n_B^{Q*} and adding the condition $T_{Q*} = T$ previously found we obtain

$$\sum_{i=B,C,S,e} Y_i^* \mu_i^H = \sum_{i=B,C,S,e} Y_i^* \mu_i^{Q*} \quad (50)$$

Thanks to those conditions, T_{Q*}, n_B^{Q*} can be fixed and all the thermodynamic quantities can be computed. The R_* that maximizes W is

$$R_* = \frac{2\sigma}{P_{Q*} - P_H}, \quad (51)$$

corresponding indeed to an (unstable) mechanical equilibrium configuration.

The work W_1 can be computed using Eq. (34), while W_2 becomes

$$W_2 = -\frac{4}{3} \pi R_*^3 \left[P_{Q*} - P_H - n_B^{Q*} \sum_{i=B,C,S,e} Y_i^* (\mu_i^H - \mu_i^{H*}) \right] + 4\pi\sigma R_*^2 \quad (52)$$

while the total work W

$$W = -\frac{4}{3} \pi R_*^3 [P_{Q*} - P_H] + 4\pi\sigma R_*^2. \quad (53)$$

By substituting Eq. (51) in Eq. (53) we obtain

$$W = \frac{16}{3} \pi \frac{\sigma^3}{(P_{Q*} - P_H)^2}. \quad (54)$$

The resulting W is the one used in [4].

To conclude this section, let us come back to the choice of $\{Y_i^*\}$. A certain subsystem of the system has a certain probability \mathcal{P}_1 to have the composition $\{Y_i^*\}$ and a deconfined quark droplet has a probability \mathcal{P}_2 to be generated in such a subsystem. Thus, complete calculations would need to compute the total nucleation probability by integrating over all the possible fluctuated composition $\{Y_i^*\}$. However, since the nucleation probability is a negative exponential of the work W , the composition associated with the lower total work

W will dominate the total probability. A good choice for $\{Y_i^*\}$, thus, will be the one that minimizes W . In [11], we assumed that such a composition is equal to the composition of a quark phase in chemical equilibrium. Namely, we have considered the fluctuation in the hadronic composition leading to a hadronic subsystem having the same composition as a quark phase in β -equilibrium $Y_i^* = Y_i^{Q\beta}$. Let us explicitly minimize W .

$$0 = \left. \frac{\partial W}{\partial Y_C^*} \right|_{n_B^{Q*}, Y_{S*}, T} = \frac{\partial}{\partial Y_C^*} \left[f_{Q*} + P_H - n_B^{Q*} \sum_{i=C,S,e} Y_i^* \mu_i^H \right] \quad (55)$$

$$= n_B^{Q*} (\mu_C^{Q*} + \mu_e^{Q*} - \mu_C^H - \mu_e^H) \quad (56)$$

where we have used Eq. (27) as constraints. Thus the condition that minimizes W with respect to Y_C^* is

$$\mu_C^{Q*} + \mu_e^{Q*} = \mu_C^H + \mu_e^H. \quad (57)$$

Similarly the condition that minimizes W with respect to Y_S^* is

$$\mu_S^{Q*} = \mu_S^H. \quad (58)$$

Note that applying those conditions to Eq. (50) together with Eqs. (25,26,27,28), we obtain

$$\mu_B^{Q*} = \mu_B^H. \quad (59)$$

One can note that Eqs. (57,58,59) corresponds to the chemical equilibrium conditions with respect to strong interactions (see e.g. [27]).

Finally, let us consider what happens when the initial hadronic phase is in β -equilibrium with neutrinos trapped (untrapped). At given n_B^H, Y_L^H, T (n_B^H, T), the β -equilibrium composition $\{Y_i^{H\beta\nu}\}$ ($\{Y_i^{H\beta}\}$) is the one that solves the equilibrium conditions

$$\mu_C^H + \mu_e^H - \mu_{\nu_e}^H = 0 \quad (\mu_C^H + \mu_e^H = 0) \quad (60)$$

$$\mu_S^H = 0 \quad (61)$$

together with the electromagnetic charge neutrality condition ($Y_C^H - Y_e^H = 0$). Replacing those conditions in Eqs. (57,58) and using Eq. (31) (Eq. (32)) we obtain

$$\mu_C^{Q*} + \mu_e^{Q*} - \mu_{\nu_e}^{H*} = \mu_C^{Q*} + \mu_e^{Q*} - \mu_{\nu_e}^{Q*} = 0 \quad (\mu_C^{Q*} + \mu_e^{Q*} = 0) \quad (62)$$

$$\mu_S^{Q*} = 0, \quad (63)$$

that, together with Eq. (27), are the conditions of β -equilibrium for quark matter (but with a different leptonic fraction with respect to the initial hadronic phase $Y_L^{Q*} \neq Y_L^H$ in the neutrino-trapped case). Thus, $Y_i^* = Y_i^{Q\beta}$ is actually the choice for $\{Y_i^*\}$ that minimizes W (and maximizes Γ) if the hadronic system is initially in neutrino-less β -equilibrium.

In conclusion, let us summarize our assumptions:

- The total nucleation probability is the product of i. the probability $\mathcal{P}_2 = \exp(-W_2/T)$ for a Q_* droplet to be formed in a H_* subsystem with the same composition $Y_i^{Q*} = Y_i^{H*} \equiv Y_i^*$ ($i = C, S$) and baryon number $N_B^{Q*} = N_B^{H*} \equiv N_B^*$ and ii. the probability $\mathcal{P}_1 = \exp(-W_1/T)$ that a subsystem H_* exists in the system H .
- Since the volume of the deconfined quark droplet is typically much smaller than the total volume $V_{Q*} \ll V$, the surroundings of the fluctuated hadronic subsystem H_* and of the quark droplet Q_* acts as thermodynamical bath (Eqs. 17,18,19)
- The composition of the quark droplet Q_* is locally conserved from the hadronic fluctuated subsystem H_* (Eqs. 25,26).

- Since the nucleation probability is proportional to a negative exponential of W/T , we consider the fluctuated composition $\{Y_i^*\}$ that minimizes W and thus will dominate the total probability (Eqs. 57, 58).
- Assuming local electromagnetic-charge neutrality in all the phases (Eq. 27, 28)
- Assuming that in the fluctuation of the hadronic composition in the subsystem H_* , the thermal and mechanical equilibrium with the surrounding are instantaneously restored (Eq. 29,30)
- Neutrinos are globally conserved and in equilibrium with the rest of the matter (if trapped) or neglected (if untrapped) (Eq. 31 or 32).
- The configuration with the critical deconfined droplet is a saddle-point configuration (Eqs. 49,50,51) (this condition can be approximately replaced with the small degrees of metastability and the thermal equilibrium between the quark droplet and the surrounding)

Given these assumptions, we found the following activation energy, namely the potential barrier height:

$$W(n_B^H, \{Y_i^H\}, T) = \frac{16\pi}{3} \frac{\sigma^3}{\left[P_Q(n_B^{Q*}, \{Y_i^{Q*}\}, T) - P_H(n_B^H, \{Y_i^H\}, T) \right]^2}, \quad (64)$$

where $n_B^{Q*}, \{Y_i^{Q*}\}$ ($i = C, S, e, \nu_e$) are fixed with

$$\mu_B^Q(n_B^{Q*}, \{Y_i^{Q*}\}, T) = \mu_B^H(n_B^H, \{Y_i^H\}, T) \quad (65)$$

$$\mu_C^Q(n_B^{Q*}, \{Y_i^{Q*}\}, T) + \mu_e^Q(n_B^{Q*}, Y_e^{Q*}, T) = \mu_C^H(n_B^H, \{Y_i^H\}, T) + \mu_e^H(n_B^H, Y_e^H, T) \quad (66)$$

$$\mu_S^Q(n_B^{Q*}, \{Y_i^{Q*}\}, T) = \mu_S^H(n_B^H, \{Y_i^H\}, T) \quad (67)$$

$$\mu_\nu^Q(n_B^{Q*}, Y_{\nu_e}^{Q*}, T) = \mu_\nu^H(n_B^H, Y_{\nu_e}^H, T) \quad (68)$$

$$Y_C^{Q*} - Y_e^{Q*} = 0. \quad (69)$$

Where Eq. (68) reduces to $Y_\nu^{Q*} = Y_\nu^H = 0$ if neutrinos are not trapped. Similarly, using the small degrees of metastability approach instead of the saddle-point approach, the activation energy is

$$W(n_B^H, \{Y_i^H\}, T) = \frac{16\pi}{3} \frac{\sigma^3}{\left\{ n_B^{Q*} \left[\mu_B^Q(n_B^{Q*}, \{Y_i^{Q*}\}, T) - \mu_B^H(n_B^H, \{Y_i^H\}, T) \right] \right\}^2}, \quad (70)$$

where $n_B^{Q*}, \{Y_i^{Q*}\}$ ($i = C, S, e$) are fixed with Eqs. (66,67,69) and

$$P_{Q*}(n_B^{Q*}, \{Y_i^{Q*}\}, T) = P_H(n_B^H, \{Y_i^H\}, T). \quad (71)$$

The thermodynamical work W_1 needed to generate the fluctuated subsystem H_* is

$$W_1(n_B^H, \{Y_i^H\}, T) = \frac{4}{3} \pi R_*^3 n_B^{Q*} \sum_{i=B,C,S,e} \left[Y_i^{Q*} \left(\mu_i^H(n_B^H, \{Y_i^H\}, T) - \mu_i^Q(n_B^{Q*}, \{Y_i^{Q*}\}, T) \right) \right], \quad (72)$$

where R_* is

$$R_*(n_B^H, \{Y_i^H\}, T) = \frac{2\sigma}{P_Q(n_B^{Q*}, \{Y_i^{Q*}\}, T) - P_H(n_B^H, \{Y_i^H\}, T)} \quad (73)$$

in the saddle-point approach, and

$$R_*(n_B^H, \{Y_i^H\}, T) = \frac{2\sigma}{n_B^{Q*} \left[\mu_B^H(n_B^H, \{Y_i^H\}, T) - \mu_B^Q(n_B^{Q*}, \{Y_i^{Q*}\}, T) \right]} \quad (74)$$

in the low-metastability approach, where $n_B^{Q*}, \{Y_i^{Q*}\}$ are computed as before and n_B^{H*} is fixed using the condition

$$P_H(n_B^{H*}, \{Y_i^{Q*}\}, T) = P_H(n_B^H, \{Y_i^H\}, T). \quad (75)$$

3. Color-superconductivity in nucleation

It has been suggested that the color-superconductivity [13] may play a fundamental role in compact stars and, in particular, that quark matter, if formed in compact stars, should be in a superconducting phase if the diquark pairing is large enough [18–20].

A fundamental point to address is the behavior of color-superconductivity in small systems, such as the first SQM droplet. Since the typical size (or coherence length) of a diquark pair is $\sim 1/\Delta$ [13], we expect a color-superconducting phase to form only in sufficiently large systems where diquark pairs have adequate space to develop (see also [43]). Thus, we will assume that the SQM will enter a CFL phase only when the droplet of SQM has a radius R larger than a specific threshold R_Δ . Within this framework, the pressure (as well as the other thermodynamic quantities) becomes radius-dependent:

$$P_Q(n_B^Q, \{Y_i^Q\}, T, R) = \begin{cases} P_{Qunp}(n_B^Q, \{Y_i^Q\}, T) & \text{if } R \leq R_\Delta \\ P_{QCFL}(n_B^Q, T) & \text{if } R > R_\Delta \end{cases}, \quad (76)$$

where the details of the unpaired and CFL EOS are reported in the Appendix A.2. In principle, one could define a smooth transition instead of such a step function. However, a smooth approach would add complexity with no particular benefits, as the results in the smooth approach could be easily achieved by adjusting the free parameters in the step approach. A natural choice for R_Δ will be the coherence length. We will thus fix $R_\Delta = \hbar c / \Delta(T)$, where $\Delta(T)$ is the temperature dependent diquark gap (see Appendix A.2.2).

This approach can be applied to situations where the energetic convenience of the bulk, compared to a finite system, arises even from factors other than surface tension. In terms of the Bag model, we can describe this possibility by assuming that the Bag parameter depends on the volume of the SQM system (or, equivalently, the baryon number). In particular, the Bag would decrease as a function of the baryon number of the system.

The critical droplet radius (Eq. 73) becomes

$$R_*(n_B^H, \{Y_i^H\}, T) = \begin{cases} R_{unp*}(n_B^H, \{Y_i^H\}, T) & \text{if } R_{unp*}(n_B^H, \{Y_i^H\}, T) \leq R_\Delta \\ \max[R_\Delta, R_{CFL*}(n_B^H, T)] & \text{if } R_{unp*}(n_B^H, \{Y_i^H\}, T) > R_\Delta \end{cases}. \quad (77)$$

4. Results and discussion

In this section, we will report and discuss the results of our analysis. The primary focus will be on discussing the qualitative and quantitative effects of thermal fluctuations on the matter composition and of the formation of color-superconducting gaps during the nucleation process in the three-flavor case. In particular, the potential barrier between the metastable hadronic phase and the stable SQM phase will be investigated using different approaches:

- unpaired+CFL: the complete framework as described in Sec. 3. The CFL phase fulfills the Witten hypothesis but it can be formed only if the SQM droplet is larger than the typical diquark coherence length $R_* \geq R_\Delta = 1/\Delta(T)$. The composition $\{Y_i^*\}$ is fluctuated with respect to the average bulk one $\{Y_i^H\}$ and it is fixed to maximize the nucleation rate Γ (all other values of $\{Y_i^*\}$ are subleading for the calculation of Γ and can be neglected) Thus, the Q_* thermodynamical quantities are fixed using Eqs. (65,66,67,68,69) for the unpaired and Eqs. (50,68) for the CFL phase.
- Unpaired: as before, but without the CFL phase. It corresponds to the case $R_\Delta \rightarrow +\infty$.

- Frozen composition: the thermal fluctuations of the hadronic composition are neglected. The Q_* thermodynamical variables are computed by fixing $Y_i^* = Y_i^H$ ($i = C, S, e$ or equivalently $i = u, d, s, e$) and Eq. (50,68). This is the approach used in [3].

In the examples reported in this section, we will use a parametrization for the CFL phase that fulfills the Witten hypothesis on absolutely stability of SQM [44,45] and a parametrization for the unpaired phase that does not lead to absolutely stable SQM, namely ($E/A_{CFL} < E/A_{56Fe} < E/A_{unp}$ in bulk at zero pressure and temperature) (see Appendix A.2). This choice allows for the existence of compact stars as massive as $\sim 2.6 M_\odot$ and which are interpreted as being CFL-QSs in the context of the two families compact stars scenario [20]. At the same time, for the unpaired phase, the potential barrier for the nucleation turns out to be large enough to shift the threshold of formation of this phase at large values of n_B^H, T to make the appearance of SQM at not too low n_B^H, T . A detailed discussion will be provided in a future work (in preparation).

However, we stress that the framework presented here can also be applied in cases in which both the CFL and unpaired SQM do not fulfill Witten's hypothesis.

Some properties of the used EOSs are reported in Fig. 1. In particular, the upper panels show the pressure as a function of the initial hadronic baryon density n_B^H at two different temperatures for the initial hadronic phase (H), for the unpaired SQM with the fluctuated composition (Q_* fluct. unp), for the unpaired SQM computed assuming a frozen composition (Q_* froz. unp) and for the CFL SQM (Q_* fluct. CFL). Note that the three Q_* pressures are not reported as a function of their baryon density n_B^{Q*} since they are computed imposing Eqs. (65,66,67,68,69) at given n_B^H and T . The favored phase is the one with the highest pressure at given n_B^H and T (see Eqs. 53, where the bulk part of W is the energy difference in bulk between the phases Q_* and H). In our scenario, the CFL phase fulfills the Witten hypothesis, and it is indeed always more stable in bulk than the hadronic phase. On the other hand, unpaired SQM does not fulfill the Witten hypothesis in our picture and becomes more stable than the hadronic phase only at high enough n_B^H and/or T . The intersection points $P_{Q*} = P_H$ correspond to the coexistence pressure of the mixed phase in bulk. If $\sigma = 0$, no finite-size effects take place and the deconfinement starts as soon as the bulk coexistence pressure is reached. However, if $\sigma \neq 0$, the critical radius R_*^{unp} diverges at $P_H = P_{Q*}$ as can be noted in Eq. (73). At the n_B^H and T at which $P_{Q*} > P_H$, the hadronic phase is metastable with respect to the Q_* phase, R_*^{unp} has a finite value, and the unpaired SQM nucleation has a finite probability to happen. The Q_* phase with the composition fluctuation that minimizes W is always energetically favorable with respect to the one with frozen composition. At fixed initial hadronic phase, with values $n_B^H, \{Y_i^H\}, T$, the total work W (Eq. 53) depends only on Q_* . Since the bulk term of W is the energy difference between the Q_* and H phases in bulk, the most stable Q_* in bulk is the one that minimizes W .

In the results presented here, the initial hadronic phase is in ν -less β -equilibrium (H_β). Note that, even if the initial hadronic phase is in equilibrium with respect to weak reactions, weak interactions do not play any role during the nucleation. Moreover, we stress that our framework can be easily applied to an initial hadronic phase with a generic composition $\{Y_i^H\}$ ($i = C, S$), not assuming any weak equilibrium. The model for computing the hadronic EOS is reported in Appendix A.1.

By increasing the temperature, the unpaired SQM pressure increases faster than the hadronic pressure, both in the fluctuated and frozen cases. This implies that the coexistence pressure is reached at a lower value of n_B^H . The behavior of the CFL pressure is not monotonic with the temperature since Δ decreases with the temperature.

The bottom panels show the hadronic composition (left) and the unpaired ⁷ Q_* composition in the fluctuated and frozen cases (right) as a function of the initial hadronic baryon density and at fixed temperature. A discussion about the roles of hyperons and deltas can be found in [8,46]. The fluctuated case, namely the composition $\{Y_i^*\}$ of the fluctuated

⁷ the CFL composition is not shown, since it is always $Y_C^* = 0$ and $Y_S^* = 1$.

subsystem associated with the lowest potential barrier height, shows very high values of Y_S^* and low values of Y_C^* as compared with the values in hadronic phase, in the low n_B^H regime. By increasing n_B^H , hyperons and deltas appear, Y_S^H (Y_C^H) increases (decreases), and the frozen composition becomes more and more similar to the fluctuated one. As noted in Sec. 2, as long as the initial hadronic phase is in β -equilibrium, the unpaired fluctuated composition corresponds to the composition of β -equilibrium SQM. This consideration applies both if neutrinos are trapped or not; however, in the former case, $Y_L^{Q*} \neq Y_L^H$. We stress again that the compositions are always reported as a function of n_B^H and not of the baryon density of the H_* nor of the Q_* phases.

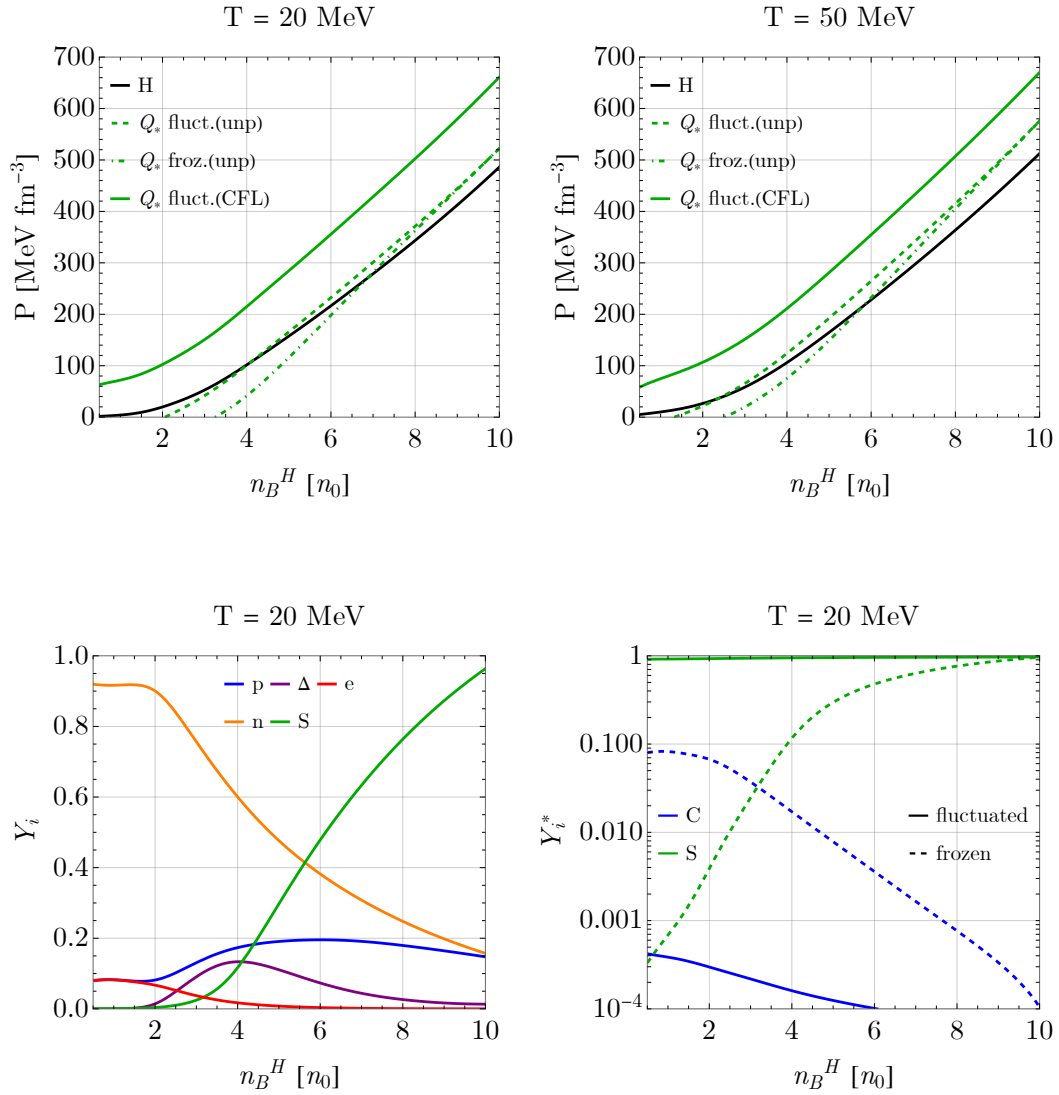


Figure 1. Top: pressure P as a function of the initial baryon density n_B^H at fixed temperature $T = 20$ MeV (left) and $T = 50$ MeV (right). The different lines refer to the hadronic phase H , unpaired SQM with the fluctuated composition (Q_* fluct. unp), unpaired SQM with the frozen composition (Q_* froz. unp) and CFL SQM (Q_* fluct. CFL). Bottom: composition of the initial hadronic phase $\{Y_i^H\}$ as a function of the initial baryon density n_B^H at fixed temperature $T = 20$ MeV (left). For an easier interpretation of the plot, hyperons are not shown separately, but the total strangeness is reported. The contribution of the deltas $\Delta^{++}, \Delta^+, \Delta^0, \Delta^-$ are summed in Δ . Composition of the first droplet of unpaired SQM in the fluctuated and frozen cases (right). The frozen composition corresponds to the initial hadronic one. The initial hadronic phase is in ν -less β -equilibrium. We fix the parameters $B_{unp}^{1/4} = 175$ MeV, $B_{CFL}^{1/4} = 135$ MeV, $\Delta_0 = 80$ MeV.

Fig. 2 displays the composition fluctuation probability ($\exp(-W_1/T)$). A complete discussion on the normalization and on the comparison with a multivariate gaussian can be found in [11]. In the left (right) panel the composition fluctuation probability is shown as a function of Y_C^* (Y_S^*) with a fixed $Y_S^* = Y_S^{H\beta}$ ($Y_C^* = Y_C^{H\beta}$). The maximum of the distributions correspond to $W_1 = 0$ MeV, namely to the average equilibrium configuration $Y_i^* = Y_i^{H\beta}$ ($i = C, S$). At $T = 0$, the thermal fluctuations are absent and the distribution is a δ -function centered at the equilibrium configuration. However, at finite temperature, a subsystem characterized by N_B^* baryons can locally have a composition different from the average equilibrium one. The higher the temperature, the higher the probability of big fluctuations in the composition (namely, the wider the distribution around the peak). Moreover, by increasing the size of the subsystem in terms of N_B^* , the distributions shrink around the maximum. This behavior is straightforward: fixing the fluctuation in terms of composition ΔY_i , the larger N_B^* , the larger the fluctuation in terms of number of particles ΔN_i . At $n_B^H = 3 n_0$ and $T = 20$ MeV assuming the initial hadronic phase to be in ν -less β -equilibrium, the average strangeness fraction is $Y_S^H \simeq 0.02$. In those conditions, the probability of having a subsystem with the composition that maximizes the rate $Y_S^* \simeq 0.9$ is very low $\exp(-W_1/T) \sim 10^{-94}$. More discussion on N_B^* and on the probabilities will be done after in this section.

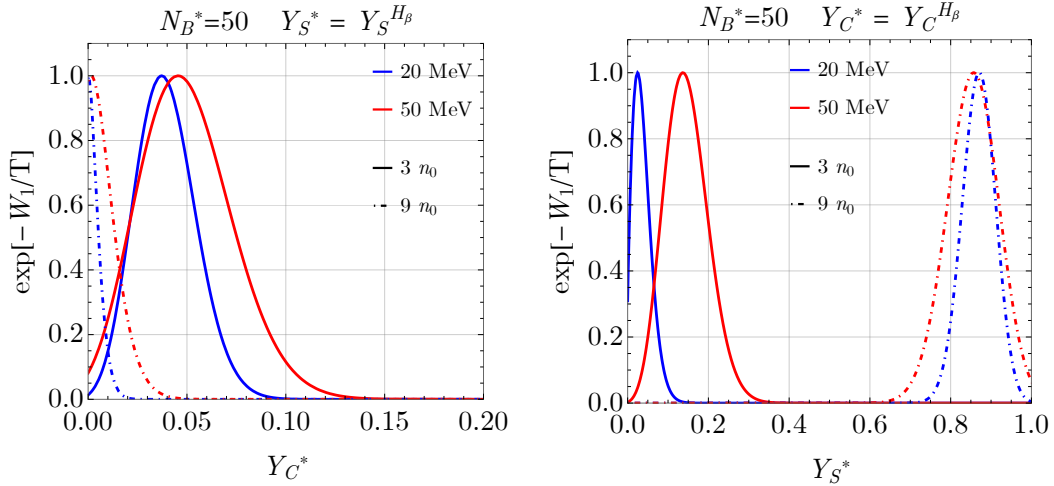


Figure 2. Non-normalized (see [11] for a discussion on the normalization) probability for a subsystem characterized by a baryon number N_B^* and in thermal and mechanical equilibrium with the surrounding to have a certain Y_C^* at fixed $Y_S^* = Y_S^{H\beta}$ (left) and a certain Y_S^* at fixed $Y_C^* = Y_C^{H\beta}$ (right). Two different temperatures T and baryon densities n_B^H are shown.

Fig. 3 shows the work needed to generate a SQM droplet as a function of the droplet radius R at fixed temperature T and initial hadronic baryon density n_B^H . The maximum of the work is reached when the system is fully in the hadronic phase, except for a critical droplet with a critical radius R_* (such that $\max[W(R)] = W(R_*)$). Such a configuration corresponds to a saddle-point, characterized by a maximum in the $W - R$ plane (unstable mechanical equilibrium point) and minima in the other independent variables (see Sec. 2). The value $W(R_*)$ can be interpreted as the potential barrier height separating the metastable hadronic phase from the stable SQM phase. In the left column panels, the different lines are obtained by computing the work using Eq. (53) but with different EOS for the SQM phase: the green line is obtained using $P_{Q*} = P_{QCFL}(n_B^{Q*}, T)$ (CFL-only), the black lines using $P_{Q*} = P_{Qunp}(n_B^{Q*}, \{Y_i^*\}, T)$ (unpaired-only) while the red lines using the framework described in Eq. (76) (unp+CFL). In this framework, for $R < R_\Delta$, the SQM

is in an unpaired phase (black and red lines are identical), since diquark pairs have not formed, as their typical coherence length ($\sim 1/\Delta$) is larger than the droplet. When $R > R_\Delta$, diquark pairs form, leading to the superconducting phase (red and green lines are identical). The critical radius in the CFL-only case R_*^{CFL} is always smaller than the unpaired-only one R_*^{unp} . We thus obtain two qualitatively different scenarios: if the critical radius in the unpaired-only case (the maximum point of the black curve) is smaller than R_Δ , the critical radius in the unp+CFL case corresponds to the unpaired-only one, and the saddle point configuration is reached before the diquark pairs have been formed ($n_B^H = 9n_0$); otherwise, if the maximum in the unpaired-only case is not reached before R_Δ ($n_B^H = 6n_0$) or not reached at all ($n_B^H = 3n_0$), diquark pairs start to form as soon as $R \geq R_\Delta$, the unp+CFL work drops to the CFL-only work, and the maximum of the work is thus at $R_* = R_\Delta$ (left panel). By choosing a larger value for Δ_0 , the R_*^{unp} is not affected, while R_Δ becomes lower, leading to a smaller R_* when $R_*^{unp} > R_\Delta$.

The dashed and dotted red lines show, respectively, W_2 , namely the work needed to generate the droplet Q_* in a subsystem H_* , and W_1 , namely the work needed to generate a hadronic subsystem H_* characterized by a fluctuated composition with respect to the average bulk value H . The work W_1 is always positive since the energy of a fluctuated hadronic configuration is always larger than the equilibrium configuration. Moreover, it monotonically increases with R since the larger the fluctuation (namely, the larger $N_B^* = n_B^{Q_*} V_{Q_*} \propto R^3$), the larger the energy difference between the fluctuated and the equilibrium configurations. On the other hand, W_2 contains two terms: the finite size term is always positive and monotonically increasing with $\propto R^2$, while the bulk term is negative (positive) and monotonically decreasing (increasing) with $\propto R^3$ if the Q_* is more (less) stable than H_* . Thus, if Q_* is more stable than H_* , W_2 is positive at low R , reaches a maximum in R_2 , and becomes negative for large R . The discontinuities at $R = R_\Delta = 1/\Delta(T)$ are due to the onset of CFL phase (which is sharp in our simplified approach). The work W_1 is smaller at $n_B^H = 9n_0$ since the difference between the composition $\{Y_i^H\}$ and $\{Y_i^{Q_*}\}$ is much smaller than the one at $n_B^H = 3n_0$ as can be easily noted in Fig. 1 and 2.

Increasing n_B^H and T at fixed R , $W \propto (P_H - P_{Q_*})$ decreases (see top panels in Fig. 1) leading to a lower activation energy $W(R_*)$ even if R_* does not change (i.e. even if $R_*^{unp} > R_\Delta$). Note that at the conditions of the top left panel ($n_B^H = 3n_0$, $T = 20$ MeV), H is not metastable with respect to the unpaired Q_* phase, thus the black line is monotonically increasing and R_*^{unp} is not defined. However, in the CFL+unp framework, nucleation is in principle still possible thanks to the onset of CFL phase at $R = R_\Delta \simeq 2.6$ fm.

The panels in the right column show the work as a function of the droplet radius for the unpaired SQM with a fluctuated (black solid line) and frozen (orange solid line) composition. Note that the black solid lines in the two columns are identical. In general, we note that the potential barrier $W(R_*^{unp})$ is always lower in the fluctuated case. At $T = 20$ MeV and $n_B^H = 3n_0$, the hadronic phase in ν -less β -equilibrium is more stable than the unpaired Q_* phase, both in fluctuated and frozen cases (see top-left panel in Fig. 1). Thus, both the solid orange and black lines are monotonically increasing and the critical radii do not exist. At $n_B^H = 6n_0$, H_β is less stable than Q_* in the fluctuated case, which is thus not monotonically increasing and has a critical radius (black dot). Finally, Q_* is more stable than H_β in both the fluctuated and frozen cases at $n_B = 9n_0$. Moreover, since in those conditions $\{Y_i^{H_\beta}\}$ is similar to the β -equilibrium unpaired SQM, then frozen and fluctuated cases are similar. The dotted and dashed lines refer to W_1 and W_2 as in the left column, but considering only unpaired SQM. Note that $W_1 = 0$ and $W_2 = W$ in the frozen composition approach. In general, the higher the surface tension σ , the higher the potential barrier. In particular, the work W at fixed R depends linearly on the surface tension $W \propto \sigma$ (see Eq. 53). The dependence of R_* and $W(R_*)$ on σ is different in the two cases $R_*^{unp} < R_\Delta$ and $R_*^{unp} > R_\Delta$. In the former case $R_* = R_*^{unp} \propto \sigma$ (see Eq. 51) and thus $W(R_*) \propto \sigma^3$ (see Eq. 54). On the other hand, in the latter case, $R_* = R_\Delta \not\propto \sigma$ and thus $W(R_*) \propto \sigma$.

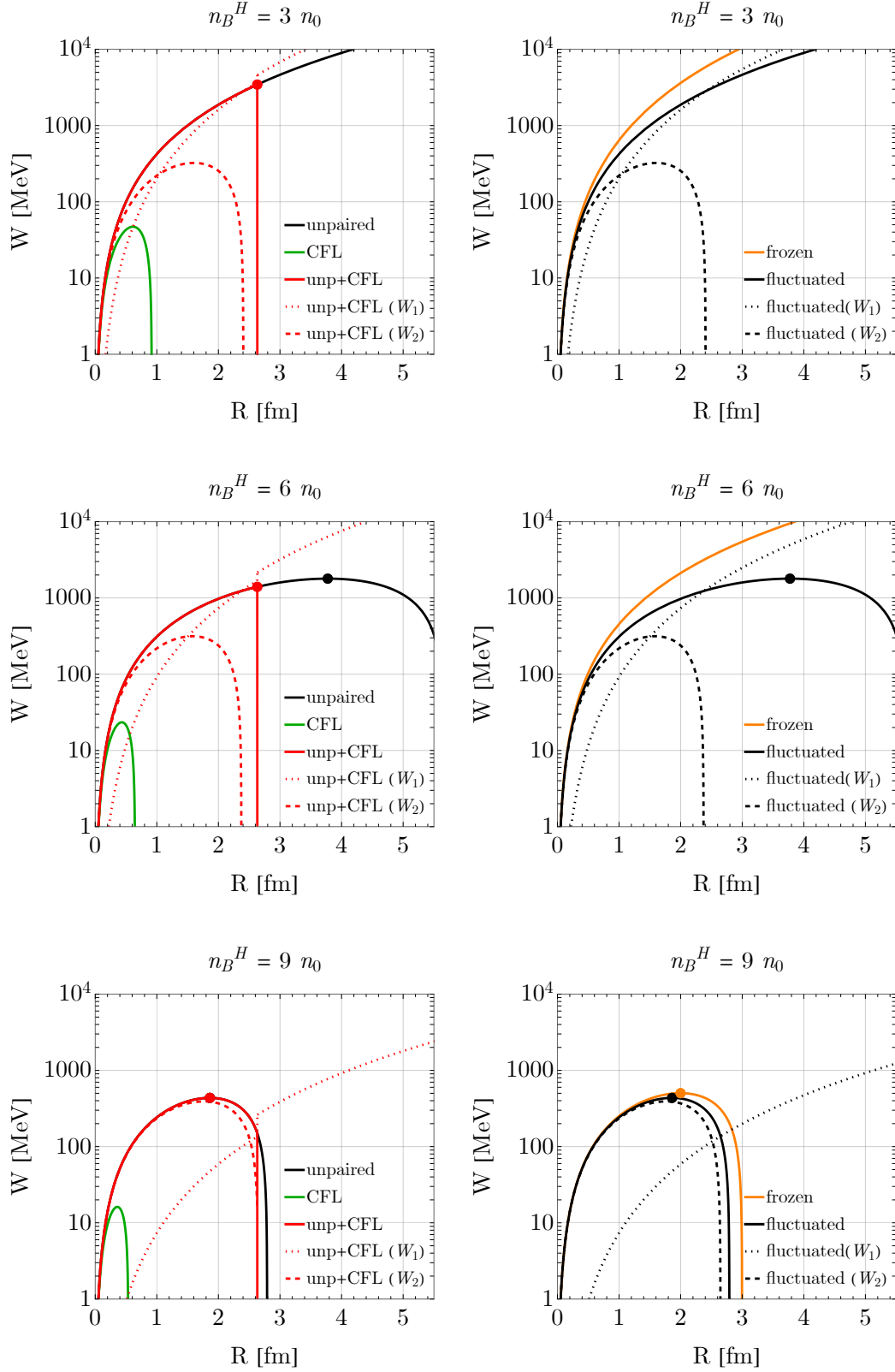


Figure 3. Work to generate a SQM droplet as a function of the radius R for $n_B^H = 3 n_0$ (top), $n_B^H = 6 n_0$ (middle) and $n_B^H = 9 n_0$ (bottom). Left column: the red line refers to the approach described in Sec. 3, the black line considers only unpaired SQM, while the green line considers only CFL SQM. The dashed and dotted lines refer respectively to W_2 (work needed to convert a subsystem H_* to Q_* with a H surrounding) and W_1 (work needed to generate a subsystem H_* in a system H). The red dot denotes the saddle point configuration, namely the critical radius R_* and the activation energy $W(R_*)$, while the black dot refers to the critical radius in the unpaired-only case R_*^{unp} . Right column: orange lines refer to the frozen composition case, while the black lines refer to the unpaired-only fluctuated composition case. The solid, dotted, and dashed black lines show W , W_1 , and W_2 in the unpaired case, respectively. The initial hadronic matter is in ν -less β -equilibrium. We set $T = 20$ MeV, $\sigma = 30$ MeV fm $^{-2}$, $\Delta_0 = 80$ MeV and $B_{unp}^{1/4} = 175$ MeV.

Finally, we provide a qualitative discussion on the order of magnitude of the potential barrier height for the conditions relevant in astrophysical systems. In particular, using Eq. (3), we note that the nucleation time is $\tau \simeq 1$ s when $W/T \simeq (165 - 180)$ for the astrophysically relevant range of n_B^H and T . This large value leads to a very low nucleation probability $\exp(-W/T) \simeq 10^{-79} - 10^{-72}$ and a very low nucleation rate $\Gamma \simeq 2 \times 10^{-52} \text{ s}^{-1} \text{ fm}^{-3}$. However, such a small rate is still enough to have a nucleation event in typically one second since the system we are considering, namely a sphere with a radius of 100 m in the compact star core, is very big $V \simeq 4 \times 10^{51} \text{ fm}^3$. In other words, even if the nucleation rate is locally very small, only one event is needed to trigger deconfinement, and in the system there are a lot of possible subsystems in which it can happen. Moreover, we note that the values of $\exp[W_1/T]$ and $\exp[W_2/T]$ leading to a nucleation time of ~ 1 s are very different by changing n_B^H, T , while their product always lead to the values of the order of magnitude reported above. For example, in the unp+CFL fluctuated approach at $n_B^H = 3 n_0$ and $\sigma = 30 \text{ MeV fm}^{-2}$, $\tau = 1$ s is obtained at $T \simeq 20 \text{ MeV}$, leading to $W/T \simeq 172$, and $\exp[-W/T] \simeq 10^{-75}$. In those conditions, we obtain $W_1/T \simeq 185$ and $W_2/T \simeq -12$. The number of baryons of the critical droplet is $N_B^* \simeq 45$. At $n_B^H = 6 n_0$, $\tau = 1$ s is reached at $T \simeq 8 \text{ MeV}$, $W/T \simeq 177$, $N_B^* \simeq 68$, $W_1/T \simeq 254$ and $W_2/T \simeq -78$. Thus, even if a certain subsystem characterized by a fluctuated composition has a very tiny probability to form (small $\exp[W_1/T]$), it could anyway appear somewhere in such a big system and its nucleation probability could be greatly enhanced by the contribution of $\exp[W_2/T]$. Thus, the total nucleation probability turns out to be much greater than the one obtained within the frozen composition approach. At fixed $n_B^H = 3 n_0$ and $\tau = 1$ s, the temperature in the unpaired-only fluctuated and frozen cases is higher than the unp+CFL approach ($T \simeq 50 \text{ MeV}$ in the unpaired-only fluctuated approach and at $T \simeq 80 \text{ MeV}$ in the unpaired frozen approach). The activation energy divided by the temperature is similar in all the cases ($W/T \simeq 170$ and $W/T \simeq 168$ respectively) even if W_2/T and W_1/T are very different for different cases and thermodynamical conditions. Increasing the n_B^H the above mentioned quantities converge to the same values for the three different approaches since the unpaired and unp+CFL approaches becomes identical when $R_*^{unp} < R_\Delta$ and the frozen approach converges to the fluctuated one when the initial average hadronic composition matches the composition of β -equilibrium SQM. A more complete analysis will be provided in a future work.

5. Summary and conclusions

The main goal of this work was to present a framework that aims to investigate the role of thermal fluctuations of the composition and of color-superconductivity in the nucleation of SQM in the typical conditions of high-energy astrophysical systems related to compact stars.

In the context of deconfinement first-order phase transitions, nucleation can be interpreted as the overcoming of the potential barrier between the metastable hadronic phase and the stable SQM phase, and it takes into account the finite-size effects and the timescale of the fluctuations.

Within the Witten hypothesis of the absolute stability of SQM and of the two families scenario of compact stars, SQM nucleation is the trigger leading to the conversion of an ordinary NS into a QS.

While a complete treatment of the nucleation process would require microphysical calculations that consider interaction rates and diffusion timescales, an approximate analysis can be performed within a thermodynamic approach. A key point is that the timescale associated with the weak interactions is much longer than that of strong interactions, which are responsible for the deconfinement phase transition. Thus, a standard approach is to impose that the newly formed quark matter droplets have the same composition as the initial hadronic phase, since weak interactions do not have sufficient time to modify the flavor composition during the nucleation.

However, this approach neglects thermal fluctuations of the composition, assuming that it is locally identical everywhere in the system. Here we present explicit thermodynamic calculations in which the total nucleation probability is computed as the product of the nucleation probability in a subsystem H_* characterized by a composition locally different from the average bulk one H , and the probability that the subsystem H_* exists in the system. This approach has already been described in our previous work [11] and has been reviewed in some parts and applied to the three flavors case here.

Within the assumptions here described (and summarized at the end of Sec. 2), we found that the first droplet of SQM has the same chemical potentials $\mu_C + \mu_e$ and μ_S of the initial hadronic phase. This also implies that if the initial hadronic phase is in β -equilibrium, also the first droplet of SQM will be in β -equilibrium, possibly with a different $Y_L^{Q*} \neq Y_L^H$, in case neutrinos are trapped. We stress that this result has been obtained even if weak interactions are not playing any role during nucleation. Thus, only finite size effects give a contribution to the potential barrier, while the chemical unbalance related to strong vs weak timescales is hidden due to thermal fluctuations of the composition.

We found that, for the typical temperatures reached in the CCSNe and PNS evolution, thermal fluctuations of the composition, in general, lower the potential barrier, leading SQM to appear at lower n_B^H and/or T . The role of thermal fluctuations becomes negligible when the composition of the initial hadronic phase is similar to the β -equilibrium SQM phase.

This result is also important for the standard one-family or twin-star scenario of compact stars, since the frozen composition approach led to a big delay, in terms of n_B^H, T , for triggering the formation of the mixed phase. On the other hand, considering the thermal fluctuations of the composition, the delay is downsized and related only to finite size effects (i.e., the surface tension), which can be easily added in a thermodynamic approach or mimicked by controlling the local/global charge neutrality.

It has been suggested that color-superconductivity could be crucial for explaining the phenomenology of compact stars, and the massive compact star observations in particular, both in hybrid stars in the standard one family scenario (see e.g. [17–19]) and in QS within the two families scenario (see e.g. [20]). Since the typical coherence length of a diquark pair is $\sim 1/\Delta$, we propose a framework in which the SQM EOS can be described as unpaired if the SQM droplet is smaller than $1/\Delta$ and as a color-superconducting phase (we have considered a CFL phase for simplicity) as soon as the quark droplet is larger than the coherence length of diquark pairs. Within this framework, the maximum QS mass (or hybrid star mass) is set by the chosen parametrization of CFL EOS, while the nucleation conditions depend on the unpaired EOS and on the diquark coherence length, and thus also on the temperature-dependent superconducting gap $R_\Delta(T) = 1/\Delta(T)$.

The qualitative results within this framework depend on whether or not the critical radius of the unpaired SQM droplet is reached before that of the diquark pairs appears (namely, if $R_*^{unp} < R_\Delta$). In particular, at high n_B^H and/or T , $R_*^{unp} < R_\Delta$, then $R_* = R_*^{unp}$ and the results with an unpaired SQM are re-obtained. On the other hand, at low n_B^H and T , $R_*^{unp} > R_\Delta$ and the maximum of W is reached as soon as diquark pairs appears, thus $R_* = R_\Delta$. Note that in the latter case, the critical radius is independent of n_B^H but depends on T since $\Delta = \Delta(T)$.

We stress again that, even if we have chosen for the examples a CFL phase that respects the Witten hypothesis, the same framework can be easily applied to hybrid stars in the one family scenario, and a similar qualitative discussion can be done.

Our calculation employs a thermodynamic approach to model the decay of a metastable state into a stable state. However, this approach could misestimate the true nucleation probabilities. For example, nucleation time could be underestimated since some microphysical mechanisms could make the composition fluctuation less likely by slowing strangeness diffusion.

Moreover, we assumed here a local electromagnetic charge neutrality, while a complete discussion should properly take into account how leptons distribute in space to screen the electric charge.

In this work, we focus on the detailed treatment of general nucleation theory and on the description of the effects of composition fluctuations and of color-superconductivity on the potential barrier. A discussion on the astrophysical implications is beyond the scope of this paper. In particular, more specific results and developments in the context of the two-families scenario will be discussed in a work in preparation in which we will also address the issue of the birth of Qs within CCSN and their subsequent PNS evolution. Moreover, we will test the robustness of our result by using a more sophisticated EOS for the SQM phase. In particular, we plan to use models for which the vacuum energy (the Bag constant in Bag-like models) and the color superconducting gap Δ are computed in a thermodynamically consistent way instead of introducing them as free parameters of the model. Some assumptions used in this work are justified only for systems much larger than the typical droplet size, such as the core of a compact star. However, by relaxing those assumptions, our general formalism can also be applied to other systems, such as the early universe or heavy ion collisions.

Author Contributions: Conceptualization, M.G., G.P, A.D. and A.L.; methodology, M.G.; validation, M.G. and A.L.; formal analysis, M.G.; investigation, M.G. and G.P.; writing—original draft preparation, M.G.; writing—review and editing, M.G., G.P, A.D. and A.L.; visualization, M.G.; supervision, G.P, A.D. and A.L.; All authors have read and agreed to the published version of the manuscript.

Funding: This research received no external funding.

Acknowledgments: The authors gratefully acknowledge the CSQCD2024 international conference of the workshop series "Compact Stars in the QCD phase diagram" held at the Yukawa Institute for Theoretical Physics in Kyoto for stimulating discussions.

Conflicts of Interest: The authors declare no conflicts of interest.

Appendix A. Equation of state

A proper QCD-based description of strongly interacting matter is currently not available since the theory is challenging to solve at finite chemical potentials. Thus, the more frequent approach is to describe the confined hadronic and deconfined quark phases separately. Since we are interested in high-energy astrophysical applications other than baryonic degrees of freedom (nucleons, hyperons, delta resonances, up, down, strange quarks and their antiparticles), we will consider the contributions of leptons (electrons, neutrinos, and their antiparticles) and thermal bosons (photons and gluons). See [42,47] for reviews on EOSs of high-energy astrophysical systems. In this section, EOS models used in the paper will be described.

Appendix A.1. Hadrons

Concerning the hadronic phase, we use a relativistic mean field model in which the strong interaction between the hadrons is mediated by the exchange of massive mesons. The general form of the Lagrangian density can be written as

$$\begin{aligned}
 \mathcal{L} = & \sum_k \bar{\psi}_k [i \gamma_\mu \partial^\mu - (M_k - g_{\sigma k} \sigma) - g_{\omega k} \gamma_\mu \omega^\mu - g_{\phi k} \gamma_\mu \phi^\mu - g_{\rho k} \gamma_\mu \vec{t} \cdot \vec{\rho}^\mu] \psi_k + \frac{1}{2} (\partial_\mu \sigma \partial^\mu \sigma - m_\sigma^2 \sigma^2) - U(\sigma) \\
 & + \frac{1}{2} m_\omega^2 \omega_\mu \omega^\mu + \frac{1}{2} m_\phi^2 \phi_\mu \phi^\mu + \frac{1}{2} m_\rho^2 \vec{\rho}_\mu \cdot \vec{\rho}^\mu + \frac{1}{4} c (g_{\omega N}^2 \omega_\mu \omega^\mu)^2 + \frac{1}{4} d (g_{\rho N}^2 \vec{\rho}_\mu \cdot \vec{\rho}^\mu)^2 + g_{\rho N}^2 A(\sigma, \omega_\mu \omega^\mu) \vec{\rho}_\mu \cdot \vec{\rho}^\mu \\
 & + \bar{\psi}_{\Delta \nu} [i \gamma_\mu \partial^\mu - (M_\Delta - g_{\sigma \Delta} \sigma) - g_{\omega \Delta} \gamma_\mu \omega^\mu - g_{\rho \Delta} \gamma_\mu I_3 \rho_3^\mu] \psi_\Delta^\nu \\
 & - \frac{1}{4} F_{\mu\nu} F^{\mu\nu} - \frac{1}{4} P_{\mu\nu} P^{\mu\nu} - \frac{1}{4} \vec{G}_{\mu\nu} \vec{G}^{\mu\nu},
 \end{aligned} \tag{A1}$$

where the sum over k runs over the full octet of the lightest baryons ($p, n, \Lambda, \Sigma^+, \Sigma^0, \Sigma^-, \Xi^0, \Xi^-$) interacting with $\sigma, \omega, \phi, \rho$ meson fields, M_k is the vacuum baryon mass of index k , $U(\sigma)$ is a nonlinear self-interaction potential of the σ meson,

$$U(\sigma) = \frac{1}{3}a (g_{\sigma N} \sigma)^3 + \frac{1}{4}b (g_{\sigma N} \sigma^4), \quad (\text{A2})$$

introduced by Boguta and Bodmer [48] to achieve a reasonable compressibility for equilibrium normal nuclear matter. Following Ref. [49,50], the nonlinear function

$$A(\sigma, \omega_\mu \omega^\mu) = \sum_{i=1}^6 a_i \sigma_i + \sum_{j=1}^3 b_j (\omega_\mu \omega^\mu)^j, \quad (\text{A3})$$

has been introduced in order to fix the experimental range of values of the symmetry energy and the symmetry energy slope L . In the third line of Eq.(A1) is reported the lagrangian density related to the Δ -isobars ($\Delta^{++}, \Delta^+, \Delta^0, \Delta^-$), where ψ_Δ^ν is the Rarita-Schwinger spinor and I_3 is the matrix containing the isospin charges [51,52]. Finally, the field strength tensors for the vector mesons are given by the usual expressions $F_{\mu\nu} \equiv \partial_\mu \omega_\nu - \partial_\nu \omega_\mu$, $P_{\mu\nu} \equiv \partial_\mu \phi_\nu - \partial_\nu \phi_\mu$, $\vec{G}_{\mu\nu} \equiv \partial_\mu \vec{\rho}_\nu - \partial_\nu \vec{\rho}_\mu$.

In the present analysis, we adopt the so-called SFHo parametrization (see [50] for details). The scalar σ meson-hyperon coupling constants have been fitted to reproduce the potential depth of the corresponding hyperon at saturation nuclear matter [53,54]

$$U_\Lambda^N = -28 \text{ MeV}, \quad U_\Sigma^N = +30 \text{ MeV}, \quad U_\Xi^N = -18 \text{ MeV}, \quad (\text{A4})$$

while, for the coupling with vector mesons, we use the SU(6) symmetry relations [53,55].

Concerning the meson- Δ coupling constants, we fix the ratio $x_{\sigma\Delta} = g_{\sigma\Delta}/g_{\sigma N} = 1.0$, $x_{\omega\Delta} = g_{\omega\Delta}/g_{\omega N} = 1.0$ and $x_{\rho\Delta} = g_{\rho\Delta}/g_{\rho N} = 1.0$. Such a choice results to be consistent with phenomenological analysis of the data relative to electron-nucleus, photoabsorption, pion nucleus scattering and with the experimental flow data of heavy-ion collisions at intermediate energies [46,56–58].

Appendix A.2. Deconfined quarks

In this work, we are interested in two deconfined quark matter phases: an unpaired quark phase and a color-superconducting phase. In particular, systems smaller (bigger) than the typical diquark pair size will be described with an unpaired (CFL) EOS (see Sec. 3). In both cases, MIT Bag models with perturbative corrections will be extended to finite temperatures.

Appendix A.2.1. Unpaired phase

The unpaired deconfined quark phase will be described using a α Bag model (a MIT Bag model with perturbative corrections to the first order) [59,60] in which the finite

temperature generalization is included as in [61]. The total baryon density, pressure, energy density, entropy density and free energy density are

$$n_B^{Qunp}(\{\mu_i\}, T) = \frac{1}{3} \sum_{i=u,d,s} n_i^Q(\mu_i, T) \quad (A5)$$

$$P_B^{Qunp}(\{\mu_i\}, T) = \sum_{i=u,d,s} P_i^Q(\mu_i, T) - B_{unp} \quad (A6)$$

$$\varepsilon_B^{Qunp}(\{\mu_i\}, T) = \sum_{i=u,d,s} \varepsilon_i^Q(\mu_i, T) + B_{unp} \quad (A7)$$

$$s_B^{Qunp}(\{\mu_i\}, T) = \sum_{i=u,d,s} s_i^Q(\mu_i, T) \quad (A8)$$

$$f_B^{Qunp}(\{\mu_i\}, T) = \varepsilon_B^{Qunp}(\{\mu_i\}, T) - T s_B^{Qunp}(\{\mu_i\}, T), \quad (A9)$$

where n_i^Q refers to the net number density (namely the difference between the quark and antiquark number densities), while P_i^Q and ε_i^Q the total pressure and energy density (namely the sum between the quark and antiquark quantities) of the quark flavor i , where quark and antiquark are considered at the chemical equilibrium with respect to pair production ($\mu_i = -\mu_{\bar{i}}$). The contributions of different flavors to the thermodynamical quantities at finite temperature and chemical potential can be analytically computed in the α Bag model only for massless quarks ($m_i = 0$) [59,62]

$$n_q(\mu_i, T, m_i = 0, \alpha_s) = \left(\mu_i T^2 + \frac{1}{\pi^2} \mu_i^3 \right) \left(1 - \frac{2\alpha_s}{\pi} \right) \quad (A10)$$

$$P_q(\mu_i, T, m_i = 0, \alpha_s) = \frac{7}{60} \pi^2 T^4 \left(1 - \frac{50\alpha_s}{21\pi} \right) + \left(\frac{1}{2} T^2 \mu_i^2 + \frac{1}{4\pi^2} \mu_i^4 \right) \left(1 - \frac{2\alpha_s}{\pi} \right) \quad (A11)$$

$$\varepsilon_q(\mu_i, T, m_i = 0, \alpha_s) = 3P_q(\mu_i, T, m_i = 0, \alpha_s) \quad (A12)$$

$$s_q(\mu_i, T, m_i = 0, \alpha_s) = \frac{7}{15} \pi^2 T^3 \left(1 - \frac{50\alpha_s}{21\pi} \right) + T \mu_i^2 \left(1 - \frac{2\alpha_s}{\pi} \right). \quad (A13)$$

that correspond to lowest-order gluon interaction corrections to the massless Fermi gas with a degeneracy factor $2_{spin} \times 3_{color} = 6$. The thermodynamical quantities at finite temperature and chemical potential for a gas of non-interacting massive quarks are the Fermi integrals

$$n_q(\mu_i, T, m_i, \alpha_s = 0) = \frac{6}{2\pi^2} \int_0^{+\infty} k^2 [\mathbf{f}(k, \mu_i, T, m_i) - \mathbf{f}(k, -\mu_i, T, m_i)] dk \quad (A14)$$

$$P_q(\mu_i, T, m_i, \alpha_s = 0) = \frac{6}{2\pi^2} \frac{1}{3} \int_0^{+\infty} \frac{k^4}{E(k, m_i)} [\mathbf{f}(k, \mu_i, T, m_i) + \mathbf{f}(k, -\mu_i, T, m_i)] dk \quad (A15)$$

$$\varepsilon_q(\mu_i, T, m_i, \alpha_s = 0) = \frac{6}{2\pi^2} \int_0^{+\infty} k^2 E(k, m_i) [\mathbf{f}(k, \mu_i, T, m_i) + \mathbf{f}(k, -\mu_i, T, m_i)] dk \quad (A16)$$

$$s_q(\mu_i, T, m_i, \alpha_s = 0) = \frac{1}{T} [P_q(\mu_i, T, m, 0) + \varepsilon_q(\mu_i, T, m, 0) - \mu n_q(\mu_i, T, m, 0)], \quad (A17)$$

where the Fermi distribution function is

$$\mathbf{f}(k, \pm\mu_i, T, m_i) = \frac{1}{e^{\frac{E(k, m_i) \mp \mu}{T}} + 1} \quad (A18)$$

and the single particle energy with a momentum k is

$$E(k, m_i) = \sqrt{k^2 + m^2}. \quad (A19)$$

In this work, the Fermi integrals will be computed numerically using the JEL scheme [63] (see also [28]). Finally, the quantities for interacting massive quarks will be computed as in [61]:

$$n_i^Q(\mu_i, T) = n_q(\mu_i, T, m_i, \alpha_s = 0) - \frac{2\alpha_s}{\pi} \left(\mu_i T^2 + \frac{1}{\pi^2} \mu_i^3 \right) \quad (\text{A20})$$

$$P_i^Q(\mu_i, T) = P_q(\mu_i, T, m_i, \alpha_s = 0) - \frac{5\pi\alpha_s}{18} T^4 - \frac{2\alpha_s}{\pi} \left(\frac{1}{2} T^2 \mu_i^2 + \frac{1}{4\pi^2} \mu_i^4 \right) \quad (\text{A21})$$

$$\varepsilon_i^Q(\mu_i, T) = \varepsilon_q(\mu_i, T, m_i, \alpha_s = 0) - \frac{15\pi\alpha_s}{18} T^4 - \frac{6\alpha_s}{\pi} \left(\frac{1}{2} T^2 \mu_i^2 + \frac{1}{4\pi^2} \mu_i^4 \right) \quad (\text{A22})$$

$$s_i^Q(\mu_i, T) = s_q(\mu_i, T, m_i, \alpha_s = 0) - \frac{10\pi\alpha_s}{9} T^3 - \frac{2\alpha_s}{\pi} T \mu_i^2. \quad (\text{A23})$$

The thermodynamical quantities can also be written using $\{n_i\}$ or $n_B, \{Y_i\}$ (where $Y_i = n_i/n_B$) as free variables. Namely,

$$(\{\mu_i\}, T) \rightarrow (\{\mu_i(n_B, Y_i, T)\}, T) \rightarrow (n_B, Y_i, T) \quad (\text{A24})$$

where $\mu_i(n_B, Y_i, T)$ is the chemical potential that solves

$$n_i^Q(\mu_i, T) = n_B Y_i. \quad (\text{A25})$$

Appendix A.2.2. Color-superconducting phase (CFL)

The color-superconducting CFL phase will be treated with an extended α Bag inspired model, in which the contribution of pairing is added to the thermodynamical quantities similarly to [12].

$$n_i^{\text{QCFL}}(\{\mu_i\}, T) = n_i^Q(\mu_i, T) + \frac{2}{\pi^2} \mu_i \Delta(T)^2 \quad (\text{A26})$$

$$n_B^{\text{QCFL}}(\{\mu_i\}, T) = \frac{1}{3} \sum_{i=u,d,s} \left[n_i^Q(\mu_i, T) + \frac{2}{\pi^2} \mu_i \Delta(T)^2 \right] \quad (\text{A27})$$

$$P_B^{\text{QCFL}}(\{\mu_i\}, T) = \sum_{i=u,d,s} P_i^Q(\mu_i, T) + \frac{1}{\pi^2} \Delta(T)^2 \sum_{i=u,d,s} \mu_i^2 - B_{\text{CFL}} \quad (\text{A28})$$

$$\varepsilon_B^{\text{QCFL}}(\{\mu_i\}, T) = f_B^{\text{QCFL}}(\{\mu_i\}, T) + T s_B^{\text{QCFL}}(\{\mu_i\}, T) \quad (\text{A29})$$

$$s_B^{\text{QCFL}}(\{\mu_i\}, T) = \sum_{i=u,d,s} s_i^Q(\mu_i, T) + \frac{2}{\pi^2} \Delta(T) \frac{\partial \Delta(T)}{\partial T} \sum_{i=u,d,s} \mu_i^2 \quad (\text{A30})$$

$$f_B^{\text{QCFL}}(\{\mu_i\}, T) = -P_B^{\text{QCFL}}(\{\mu_i\}, T) + \sum_i \mu_i n_i^{\text{QCFL}}(\{\mu_i\}, T), \quad (\text{A31})$$

where $\Delta(T)$ is a finite temperature extension of the gap parameter [13,64]

$$\Delta(T) = \Theta(T_c - T) \Delta_0 \sqrt{1 - \frac{T}{T_c}}, \quad (\text{A32})$$

where Δ_0 is the gap parameter at zero temperature, and $T_c \simeq 2^{1/3} 0.57 \Delta_0$ [13,64]. Differently with respect to the unpaired case, in CFL phase, the chemical potentials $\{\mu_i\}$ are not free variables but are fixed by the conditions that number densities of up, down and strange quarks are equal. Namely,

$$(\{\mu_i\}, T) \rightarrow (\{\mu_i(n_B, T)\}, T) \rightarrow (n_B, T) \quad i = u, d, s \quad (\text{A33})$$

using

$$n_u^{\text{QCFL}}(\{\mu_i\}, T) = n_d^{\text{QCFL}}(\{\mu_i\}, T) = n_s^{\text{QCFL}}(\{\mu_i\}, T) \quad (\text{A34})$$

Appendix A.3. Leptons

Electrons and positrons will be treated as massive non-interacting Fermi gas with a degeneracy of 2:

$$n_e(\mu_e, T) = \frac{2}{2\pi^2} \int_0^{+\infty} k^2 [\mathbf{f}(k, \mu_e, T, m_e) - \mathbf{f}(k, -\mu_e, T, m_e)] dk \quad (\text{A35})$$

$$P_e(\mu_e, T) = \frac{2}{2\pi^2} \frac{1}{3} \int_0^{+\infty} \frac{k^4}{E(k, m_e)} [\mathbf{f}(k, \mu_e, T, m_e) + \mathbf{f}(k, -\mu_e, T, m_e)] dk \quad (\text{A36})$$

$$\varepsilon_e(\mu_e, T) = \frac{2}{2\pi^2} \int_0^{+\infty} k^2 E(k, m_e) [\mathbf{f}(k, \mu_e, T, m_e) + \mathbf{f}(k, -\mu_e, T, m_e)] dk \quad (\text{A37})$$

$$s_e(\mu_e, T) = \frac{1}{T} [P_e(\mu_e, T) + \varepsilon_e(\mu_e, T) - \mu_e n_e(\mu_e, T)]. \quad (\text{A38})$$

Again, the Fermi integrals will be computed numerically using the JEL scheme [63]. Neutrinos will be treated as massless non-interacting Fermi gas with a degeneracy of 1:

$$n_\nu(\mu_\nu, T) = \frac{1}{6} \left(\mu_\nu T^2 + \frac{1}{\pi^2} \mu_\nu^3 \right) \quad (\text{A39})$$

$$P_\nu(\mu_\nu, T) = \frac{1}{6} \left(\frac{7}{60} \pi^2 T^4 + \frac{1}{2} T^2 \mu_\nu^2 + \frac{1}{4\pi^2} \mu_\nu^4 \right) \quad (\text{A40})$$

$$\varepsilon_\nu(\mu_\nu, T) = 3P_\nu(\mu_\nu, T) \quad (\text{A41})$$

$$s_\nu(\mu_\nu, T) = \frac{1}{6} \left(\frac{7}{15} \pi^2 T^3 + T \mu_\nu^2 \right), \quad (\text{A42})$$

As for the quark phase, the thermodynamical quantities of electrons (neutrinos) can be written in terms of n_e, T (n_ν, T) as independent variables. Muons could also, in principle, play a role in high-energy astrophysical systems (see e.g. [65]), at least in the hadronic phase. However, in this work, they will be neglected.

Appendix A.4. Bosons

Photons will be treated as an ideal bosons gas with zero chemical potential (i.e. as a blackbody radiation):

$$P_\gamma(T) = \frac{\pi^2}{45} T^4 \quad (\text{A43})$$

$$\varepsilon_\gamma(T) = 3P_\gamma(T) \quad (\text{A44})$$

$$s_\gamma(T) = \frac{4\pi^2}{45} T^3. \quad (\text{A45})$$

The contribution of thermal gluons is [62]

$$P_g(T) = \frac{8\pi^2}{45} T^4 \left(1 - \frac{15\alpha_s}{4\pi} \right) \quad (\text{A46})$$

$$\varepsilon_g(T) = 3P_g(T) \quad (\text{A47})$$

$$s_g(T) = \frac{32\pi^2}{45} T^3 \left(1 - \frac{15\alpha_s}{4\pi} \right). \quad (\text{A48})$$

Appendix A.5. Total EOS

The total thermodynamical quantities in the hadronic and quark phases are:

$$X_H(n_B, \{Y_i\}, T) = X_B^H(n_B, \{Y_h\}, T) + X_e(n_B Y_e, T) + X_v(n_B Y_{v_e}, T) + 2X_v(0, T) + X_\gamma(T) \quad (\text{A49})$$

$$X_{Qunp}(n_B, \{Y_i\}, T) = X_B^{Qunp}(n_B, \{Y_q\}, T) + X_e(n_B Y_e, T) + X_v(n_B Y_{v_e}, T) + 2X_v(0, T) + X_\gamma(T) + X_g(T) \quad (\text{A50})$$

$$X_{QCFL}(n_B, T) = X_B^{QCFL}(n_B, T) + X_v(n_B Y_{v_e}, T) + 2X_v(0, T) + X_\gamma(T) + X_g(T), \quad (\text{A51})$$

where $X = P, \varepsilon, s, f$. In principle, the number densities $n_B, \{Y_i\}$ (or the chemical potentials $\{\mu_i\}$) are free variables. However, they can be fixed using some conditions of the system. For example, if an unpaired quark phase is in weak equilibrium and charge neutral, the five relations

$$\mu_u(n_B, \{Y_i\}, T) + \mu_e(n_B, \{Y_i\}, T) = \mu_d(n_B, \{Y_i\}, T) + \mu_{v_e}(n_B, \{Y_i\}, T) \quad (\text{A52})$$

$$\mu_d(n_B, \{Y_i\}, T) = \mu_s(n_B, \{Y_i\}, T) \quad (\text{A53})$$

$$1 = \frac{1}{3}Y_u + \frac{1}{3}Y_d + \frac{1}{3}Y_s \quad (\text{A54})$$

$$0 = \frac{2}{3}Y_u - \frac{1}{3}Y_d - \frac{1}{3}Y_s - Y_e \quad (\text{A55})$$

$$Y_L = Y_e + Y_{v_e}, \quad (\text{A56})$$

can be used to fix $Y_u, Y_d, Y_s, Y_e, Y_{v_e}$ and n_B, Y_L, T remain as independent variables.

In this work we will fix $\alpha_s = \pi/2 \times 0.1$, $m_s = 100$ MeV, $m_u = m_d = 0$, $B_{unp}^{1/4} = 175$ MeV, $B_{unp}^{1/4} = 135$ MeV and $\Delta_0 = 80$ MeV. These parameters are chosen in order to have a CFL (unpaired) phase that fullfill (does not fullfill) the Witten hypothesis on absolute stability of SQM [44,45]. In particular, the CFL parametrization is similar to the one used in [20] in the context of the two families scenario of compact stars, while the Bag of the unpaired phase is of the same order of the one used in works using unpaired deconfined quark matter (see e.g. [11,28,61,66,67]). A more detailed discussion on the astrophysical implications will be discussed in a future work. Some possible explanations for a different Bag for the unpaired and color-superconducting phases will be investigated in future works by computing the Bag and the gap for the two phases consistently, without considering them as free variables. For example, different B for different Δ_0 are obtained in [17,18], where a color-superconducting phase is computed with an NJL-like model, and then fitted in a Bag-like model [12].

However, we stress that the framework presented here can also be applied in cases in which both the CFL and unpaired SQM do not fulfill Witten's hypothesis.

References

1. Olesen, M.L.; Madsen, J. Nucleation of quark matter bubbles in neutron stars. *Phys. Rev. D* **1994**, *49*, 2698–2702, [astro-ph/9401002]. <https://doi.org/10.1103/PhysRevD.49.2698>.
2. Heiselberg, H. Quark Matter Droplet Formation in Neutron Stars, 1995, [arXiv:hep-ph/9501374].
3. Bombaci, I.; Logoteta, D.; Vidaña, I.; Providência, C. Quark matter nucleation in neutron stars and astrophysical implications. *Eur. Phys. J. A* **2016**, *52*, 58, [arXiv:astro-ph.HE/1601.04559]. <https://doi.org/10.1140/epja/i2016-16058-5>.
4. Mintz, B.W.; Fraga, E.S.; Pagliara, G.; Schaffner-Bielich, J. Nucleation of quark matter in protonneutron star matter. *Phys. Rev. D* **2010**, *81*, 123012, [arXiv:hep-ph/0910.3927]. <https://doi.org/10.1103/PhysRevD.81.123012>.
5. Iida, K.; Sato, K. Quantum nucleation of two flavor quark matter in neutron stars. *Prog. Theor. Phys.* **1997**, *98*, 277–282, [astro-ph/9705211]. <https://doi.org/10.1143/PTP.98.277>.
6. Bombaci, I.; Lugones, G.; Vidana, I. Effects of color superconductivity on the nucleation of quark matter in neutron stars. *Astron. Astrophys.* **2007**, *462*, 1017–1022, [astro-ph/0603644]. <https://doi.org/10.1051/0004-6361:20065259>.
7. Blacker, S.; Bastian, N.U.F.; Bauswein, A.; Blaschke, D.B.; Fischer, T.; Oertel, M.; Soutanis, T.; Typel, S. Constraining the onset density of the hadron-quark phase transition with gravitational-wave observations. *Phys. Rev. D* **2020**, *102*, 123023, [arXiv:astro-ph.HE/2006.03789]. <https://doi.org/10.1103/PhysRevD.102.123023>.
8. Drago, A.; Lavagno, A.; Pagliara, G. Can very compact and very massive neutron stars both exist? *Phys. Rev. D* **2014**, *89*, 043014, [arXiv:nucl-th/1309.7263]. <https://doi.org/10.1103/PhysRevD.89.043014>.

9. Drago, A.; Lavagno, A.; Pagliara, G.; Pigato, D. The scenario of two families of compact stars: 1. Equations of state, mass-radius relations and binary systems. *Eur. Phys. J. A* **2016**, *52*, 40, [arXiv:astro-ph.SR/1509.02131]. <https://doi.org/10.1140/epja/i2016-16040-3>.
10. Drago, A.; Pagliara, G. The scenario of two families of compact stars: 2. Transition from hadronic to quark matter and explosive phenomena. *Eur. Phys. J. A* **2016**, *52*, 41, [arXiv:astro-ph.SR/1509.02134]. <https://doi.org/10.1140/epja/i2016-16041-2>.
11. Guerrini, M.; Pagliara, G.; Drago, A.; Lavagno, A. Thermal Fluctuations of Matter Composition and Quark Nucleation in Compact Stars. *Astrophys. J.* **2024**, *974*, 45, [arXiv:nucl-th/2404.06463]. <https://doi.org/10.3847/1538-4357/ad67cc>.
12. Alford, M.; Braby, M.; Paris, M.; Reddy, S. Hybrid Stars that Masquerade as Neutron Stars. *The Astrophysical Journal* **2005**, *629*, 969–978. <https://doi.org/10.1086/430902>.
13. Alford, M.G.; Schmitt, A.; Rajagopal, K.; Schäfer, T. Color superconductivity in dense quark matter. *Rev. Mod. Phys.* **2008**, *80*, 1455–1515, [arXiv:hep-ph/0709.4635]. <https://doi.org/10.1103/RevModPhys.80.1455>.
14. Alford, M.G.; Rajagopal, K.; Reddy, S.; Wilczek, F. The Minimal CFL nuclear interface. *Phys. Rev. D* **2001**, *64*, 074017, [hep-ph/0105009]. <https://doi.org/10.1103/PhysRevD.64.074017>.
15. Abbott, R.; Abbott, T.D.; Abraham, S.; Acernese, F.; Ackley, K.; Adams, C.; Adhikari, R.X.; Adya, V.B.; Affeldt, C.; Agathos, M.; et al. GW190814: Gravitational Waves from the Coalescence of a 23 Solar Mass Black Hole with a 2.6 Solar Mass Compact Object. *The Astrophysical Journal Letters* **2020**, *896*, L44. <https://doi.org/10.3847/2041-8213/ab960f>.
16. Romani, R.W.; Kandel, D.; Filippenko, A.V.; Brink, T.G.; Zheng, W. PSR J0952–0607: The Fastest and Heaviest Known Galactic Neutron Star. *Astrophys. J. Lett.* **2022**, *934*, L17, [arXiv:astro-ph.HE/2207.05124]. <https://doi.org/10.3847/2041-8213/ac8007>.
17. Gärtlein, C.; Ivanytskyi, O.; Sagun, V.; Blaschke, D. Hybrid star phenomenology from the properties of the special point. *Phys. Rev. D* **2023**, *108*, 114028, [arXiv:nucl-th/2301.10765]. <https://doi.org/10.1103/PhysRevD.108.114028>.
18. Blaschke, D.; Shukla, U.; Ivanytskyi, O.; Liebing, S. Effect of color superconductivity on the mass of hybrid neutron stars in an effective model with perturbative QCD asymptotics. *Phys. Rev. D* **2023**, *107*, 063034, [arXiv:nucl-th/2212.14856]. <https://doi.org/10.1103/PhysRevD.107.063034>.
19. Ivanytskyi, O.; Blaschke, D.; Fischer, T.; Bauswein, A. Early deconfinement of asymptotically conformal color-superconducting quark matter in neutron stars. *EPJ Web Conf.* **2022**, *274*, 07010, [arXiv:nucl-th/2211.12730]. <https://doi.org/10.1051/epjconf/202227407010>.
20. Bombaci, I.; Drago, A.; Logoteta, D.; Pagliara, G.; Vidaña, I. Was GW190814 a Black Hole–Strange Quark Star System? *Phys. Rev. Lett.* **2021**, *126*, 162702, [arXiv:nucl-th/2010.01509]. <https://doi.org/10.1103/PhysRevLett.126.162702>.
21. Landau, L.; Lifshitz, E.; L.P., P. *Statistical Physics, Vol. 5*; Editori Riuniti, 1978.
22. Langer, J.S. Statistical theory of the decay of metastable states. *Annals Phys.* **1969**, *54*, 258–275. [https://doi.org/10.1016/0003-4916\(69\)90153-5](https://doi.org/10.1016/0003-4916(69)90153-5).
23. Langer, J.S.; Turski, L.A. Hydrodynamic Model of the Condensation of a Vapor near Its Critical Point. *Phys. Rev. A* **1973**, *8*, 3230–3243. <https://doi.org/10.1103/PhysRevA.8.3230>.
24. Iida, K.; Sato, K. Effects of hyperons on the dynamical deconfinement transition in cold neutron star matter. *Phys. Rev. C* **1998**, *58*, 2538–2559, [nucl-th/9808056]. <https://doi.org/10.1103/PhysRevC.58.2538>.
25. Glendenning, N.K. First order phase transitions with more than one conserved charge: Consequences for neutron stars. *Phys. Rev. D* **1992**, *46*, 1274–1287. <https://doi.org/10.1103/PhysRevD.46.1274>.
26. Muller, H. The Deconfinement phase transition in asymmetric matter. *Nucl. Phys. A* **1997**, *618*, 349–370, [nucl-th/9701035]. [https://doi.org/10.1016/S0375-9474\(97\)00018-3](https://doi.org/10.1016/S0375-9474(97)00018-3).
27. Hempel, M.; Pagliara, G.; Schaffner-Bielich, J. Conditions for Phase Equilibrium in Supernovae, Proto-Neutron and Neutron Stars. *Phys. Rev. D* **2009**, *80*, 125014, [arXiv:astro-ph.HE/0907.2680]. <https://doi.org/10.1103/PhysRevD.80.125014>.
28. Constantinou, C.; Guerrini, M.; Zhao, T.; Prakash, M. Framework for phase transitions between the Maxwell and Gibbs constructions at finite temperature. *in preparation* **2025**.
29. Greiner, C.; Koch, P.; Stoecker, H. Separation of Strangeness from Antistrangeness in the Phase Transition from Quark to Hadron Matter: Possible Formation of Strange Quark Matter in Heavy Ion Collisions. *Phys. Rev. Lett.* **1987**, *58*, 1825–1828. <https://doi.org/10.1103/PhysRevLett.58.1825>.
30. Greiner, C.; Stoecker, H. Distillation and survival of strange quark matter droplets in ultrarelativistic heavy ion collisions. *Phys. Rev. D* **1991**, *44*, 3517–3529. <https://doi.org/10.1103/PhysRevD.44.3517>.
31. Lavagno, A.; Pigato, D. Strangeness thermodynamic instabilities in hot and dense nuclear matter. *Eur. Phys. J. A* **2022**, *58*, 237, [arXiv:nucl-th/2301.06909]. <https://doi.org/10.1140/epja/s10050-022-00885-6>.
32. Di Toro, M.; Drago, A.; Gaitanos, T.; Greco, V.; Lavagno, A. Testing deconfinement at high isospin density. *Nucl. Phys. A* **2006**, *775*, 102–126, [nucl-th/0602052]. <https://doi.org/10.1016/j.nuclphysa.2006.04.007>.
33. Norsen, T. Strangeness nucleation in neutron star matter. *Phys. Rev. C* **2002**, *65*, 045805, [astro-ph/0201126]. <https://doi.org/10.1103/PhysRevC.65.045805>.
34. Heiselberg, H.; Pethick, C.J.; Staubo, E.F. Quark matter droplets in neutron stars. *Phys. Rev. Lett.* **1993**, *70*, 1355–1359. <https://doi.org/10.1103/PhysRevLett.70.1355>.
35. Palhares, L.F.; Fraga, E.S. Droplets in the cold and dense linear sigma model with quarks. *Phys. Rev. D* **2010**, *82*, 125018, [arXiv:hep-ph/1006.2357]. <https://doi.org/10.1103/PhysRevD.82.125018>.

36. Lugones, G.; Grunfeld, A.G. Surface tension of hot and dense quark matter under strong magnetic fields. *Phys. Rev. C* **2019**, *99*, 035804, [arXiv:astro-ph.HE/1811.09954]. <https://doi.org/10.1103/PhysRevC.99.035804>.
37. Fraga, E.S.; Hippert, M.; Schmitt, A. Surface tension of dense matter at the chiral phase transition. *Phys. Rev. D* **2019**, *99*, 014046, [arXiv:hep-ph/1810.13226]. <https://doi.org/10.1103/PhysRevD.99.014046>.
38. Schmitt, A. Chiral pasta: Mixed phases at the chiral phase transition. *Phys. Rev. D* **2020**, *101*, 074007, [arXiv:hep-ph/2002.01451]. <https://doi.org/10.1103/PhysRevD.101.074007>.
39. Ju, M.; Wu, X.; Ji, F.; Hu, J.; Shen, H. Hadron-quark mixed phase in the quark-meson coupling model. *Phys. Rev. C* **2021**, *103*, 025809, [arXiv:nucl-th/2102.12276]. <https://doi.org/10.1103/PhysRevC.103.025809>.
40. Bombaci, I.; Lugones, G.; Vidaña, I. Effects of color superconductivity on the nucleation of quark matter in neutron stars. *Astronomy & Astrophysics* **2006**, *462*, 1017–1022. <https://doi.org/10.1051/0004-6361:20065259>.
41. Voskresensky, D.; Yasuhira, M.; Tatsumi, T. Charge screening at first order phase transitions and hadron–quark mixed phase. *Nuclear Physics A* **2003**, *723*, 291–339. [https://doi.org/10.1016/s0375-9474\(03\)01313-7](https://doi.org/10.1016/s0375-9474(03)01313-7).
42. Oertel, M.; Hempel, M.; Klähn, T.; Typel, S. Equations of state for supernovae and compact stars. *Reviews of Modern Physics* **2017**, *89*. <https://doi.org/10.1103/revmodphys.89.015007>.
43. Amore, P.; Birse, M.C.; McGovern, J.A.; Walet, N.R. Color superconductivity in finite systems. *Phys. Rev. D* **2002**, *65*, 074005. <https://doi.org/10.1103/PhysRevD.65.074005>.
44. Witten, E. Cosmic Separation of Phases. *Phys. Rev. D* **1984**, *30*, 272–285. <https://doi.org/10.1103/PhysRevD.30.272>.
45. Bodmer, A.R. Collapsed nuclei. *Phys. Rev. D* **1971**, *4*, 1601–1606. <https://doi.org/10.1103/PhysRevD.4.1601>.
46. Drago, A.; Lavagno, A.; Pagliara, G.; Pigato, D. Early appearance of Δ isobars in neutron stars. *Phys. Rev. C* **2014**, *90*, 065809, [arXiv:astro-ph.SR/1407.2843]. <https://doi.org/10.1103/PhysRevC.90.065809>.
47. Typel, S.; et al. CompOSE Reference Manual. *Eur. Phys. J. A* **2022**, *58*, 221, [arXiv:astro-ph.HE/2203.03209]. <https://doi.org/10.1140/epja/s10050-022-00847-y>.
48. Boguta, J.; Bodmer, A.R. Relativistic Calculation of Nuclear Matter and the Nuclear Surface. *Nucl. Phys. A* **1977**, *292*, 413–428. [https://doi.org/10.1016/0375-9474\(77\)90626-1](https://doi.org/10.1016/0375-9474(77)90626-1).
49. Steiner, A.W.; Prakash, M.; Lattimer, J.M.; Ellis, P.J. Isospin asymmetry in nuclei and neutron stars. *Phys. Rept.* **2005**, *411*, 325–375, [nucl-th/0410066]. <https://doi.org/10.1016/j.physrep.2005.02.004>.
50. Steiner, A.W.; Hempel, M.; Fischer, T. Core-collapse supernova equations of state based on neutron star observations. *Astrophys. J.* **2013**, *774*, 17, [arXiv:astro-ph.SR/1207.2184]. <https://doi.org/10.1088/0004-637X/774/1/17>.
51. Li, Z.X.; Mao, G.J.; Zhuo, Y.Z.; Greiner, W. Transition to Delta matter from hot, dense nuclear matter within a relativistic mean field formulation of the nonlinear sigma and omega model. *Phys. Rev. C* **1997**, *56*, 1570–1575. <https://doi.org/10.1103/PhysRevC.56.1570>.
52. Lavagno, A. Hot and dense hadronic matter in an effective mean field approach. *Phys. Rev. C* **2010**, *81*, 044909, [arXiv:nucl-th/1004.0822]. <https://doi.org/10.1103/PhysRevC.81.044909>.
53. Schaffner, J.; Dover, C.B.; Gal, A.; Greiner, C.; Stoecker, H. Strange hadronic matter. *Phys. Rev. Lett.* **1993**, *71*, 1328–1331. <https://doi.org/10.1103/PhysRevLett.71.1328>.
54. Schaffner, J.; Mishustin, I.N. Hyperon rich matter in neutron stars. *Phys. Rev. C* **1996**, *53*, 1416–1429, [nucl-th/9506011]. <https://doi.org/10.1103/PhysRevC.53.1416>.
55. Fortin, M.; Oertel, M.; Providência, C. Hyperons in hot dense matter: what do the constraints tell us for equation of state? *Publications of the Astronomical Society of Australia* **2018**, *35*. <https://doi.org/10.1017/pasa.2018.32>.
56. Oset, E.; Salcedo, L.L. Δ Selfenergy in Nuclear Matter. *Nucl. Phys. A* **1987**, *468*, 631–652. [https://doi.org/10.1016/0375-9474\(87\)90185-0](https://doi.org/10.1016/0375-9474(87)90185-0).
57. Alberico, W.M.; Gervino, G.; Lavagno, A. Phenomenological approach to baryon resonance damping in nuclei. *Phys. Lett. B* **1994**, *321*, 177–182. [https://doi.org/10.1016/0370-2693\(94\)90460-X](https://doi.org/10.1016/0370-2693(94)90460-X).
58. Danielewicz, P.; Lacey, R.; Lynch, W.G. Determination of the equation of state of dense matter. *Science* **2002**, *298*, 1592–1596, [nucl-th/0208016]. <https://doi.org/10.1126/science.1078070>.
59. Farhi, E.; Jaffe, R.L. Strange matter. *Phys. Rev. D* **1984**, *30*, 2379–2390. <https://doi.org/10.1103/PhysRevD.30.2379>.
60. Weissenborn, S.; Sagert, I.; Pagliara, G.; Hempel, M.; Schaffner-Bielich, J. Quark Matter In Massive Neutron Stars. *Astrophys. J. Lett.* **2011**, *740*, L14, [arXiv:astro-ph.HE/1102.2869]. <https://doi.org/10.1088/2041-8205/740/1/L14>.
61. Fischer, T.; Sagert, I.; Pagliara, G.; Hempel, M.; Schaffner-Bielich, J.; Rauscher, T.; Thielemann, F.K.; Käppeli, R.; Martínez-Pinedo, G.; Liebendörfer, M. CORE-COLLAPSE SUPERNOVA EXPLOSIONS TRIGGERED BY A QUARK-HADRON PHASE TRANSITION DURING THE EARLY POST-BOUNCE PHASE. *The Astrophysical Journal Supplement Series* **2011**, *194*, 39. <https://doi.org/10.1088/0067-0049/194/2/39>.
62. Glendenning, N.K. *Compact Stars*; Astronomy and astrophysics library, Springer: New York, NY, 2012.
63. Johns, S.M.; Ellis, P.J.; Lattimer, J.M. Numerical Approximation to the Thermodynamic Integrals. *The Astrophysical Journal* **1996**, *473*, 1020. <https://doi.org/10.1086/178212>.
64. Schmitt, A. *Dense Matter in Compact Stars*; Springer Berlin Heidelberg, 2010. <https://doi.org/10.1007/978-3-642-12866-0>.
65. Loffredo, E.; Perego, A.; Logoteta, D.; Branchesi, M. Muons in the aftermath of neutron star mergers and their impact on trapped neutrinos. *Astron. Astrophys.* **2023**, *672*, A124, [arXiv:astro-ph.HE/2209.04458]. <https://doi.org/10.1051/0004-6361/202244927>.

-
66. Constantinou, C.; Han, S.; Jaikumar, P.; Prakash, M. g modes of neutron stars with hadron-to-quark crossover transitions. *Phys. Rev. D* **2021**, *104*, 123032, [[arXiv:astro-ph.HE/2109.14091](#)]. <https://doi.org/10.1103/PhysRevD.104.123032>.
 67. Constantinou, C.; Zhao, T.; Han, S.; Prakash, M. Framework for phase transitions between the Maxwell and Gibbs constructions. *Phys. Rev. D* **2023**, *107*, 074013, [[arXiv:nucl-th/2302.04289](#)]. <https://doi.org/10.1103/PhysRevD.107.074013>.

Disclaimer/Publisher's Note: The statements, opinions and data contained in all publications are solely those of the individual author(s) and contributor(s) and not of MDPI and/or the editor(s). MDPI and/or the editor(s) disclaim responsibility for any injury to people or property resulting from any ideas, methods, instructions or products referred to in the content.